



Determination of the configuration in six-membered saturated heterocycles (N, P, S, Se) and their oxidation products using experimental and calculated NMR chemical shifts



Miloš Buděšínský^{a,*}, Václav Vaněk^a, Martin Dračínský^a, Radek Pohl^a,
Lenka Poštová-Slavětínská^a, Vladimír Sychrovský^a, Jan Pícha^a, Ivana Císařová^b

^a Institute of Organic Chemistry and Biochemistry, Academy of Sciences of the Czech Republic, Flemingovo 2, CZ-166 10 Prague 6, Czech Republic

^b Department of Inorganic Chemistry, Charles University, Hlavova 2040, CZ-128 40 Prague 2, Czech Republic

ARTICLE INFO

Article history:

Received 8 January 2014
Received in revised form 2 April 2014
Accepted 14 April 2014
Available online 19 April 2014

Keywords:

Six-membered saturated heterocycles (N,P,S,Se)
Oxidation products
Configuration
NMR
Quantum chemical calculations
X-ray structures

ABSTRACT

The six-membered saturated heterocycles—4-*tert*-butyl-1-methylpiperidine, 4-*tert*-butyl-1-methylphosphine, 4-*tert*-butyl-tetrahydro-2*H*-thiopyran, and 4-*tert*-butyl-tetrahydro-2*H*-selenopyran—were prepared as suitable model compounds with well-defined geometry for an NMR study of their oxidation products. The corresponding epimeric *N*-oxides, phosphinoxides, sulfoxides, and selenoxides were obtained by standard chemical preparation and also by in situ oxidation with *meta*-chloroperbenzoic acid directly in the NMR tube. The experimental ¹H and ¹³C chemical shifts were compared with corresponding calculated data obtained by GIAO approach with DFT, MP2, and HF methods and various basis sets. The correlation of experimental versus calculated data showed the possibility to determine the stereochemistry of the epimeric oxidation products using fast DFT B3LYP/6-31G* method for both geometry optimization and NMR chemical shifts calculation.

© 2014 Elsevier Ltd. All rights reserved.

1. Introduction

It is well known that the stereochemistry of a compound pre-defines its molecular properties, such as reactivity or biological activity. Therefore, the assignment of the configuration is one of the key steps of the structure elucidation. There are several NMR methods enabling relative configuration determination. The classical approach employs NOEs¹ of spatially closed nuclei and/or certain spin-spin coupling constants, which are related to the stereochemistry (most often vicinal coupling constants and Karplus relationship² to the torsion angle of the interacting nuclei). However, for some types of chiral functional groups these NMR parameters are not accessible and configuration of these functional groups can be elucidated only indirectly (e.g., by Aromatic Solvent Induced Shift (ASIS) or by interaction of the substrate with NMR shift reagents). Another approach that has become attractive in the last two decades, is a correlation of calculated NMR parameters with observed ones.³ In combination with the probability calculation this approach seems to be powerful even in the cases when

NMR data of only one diastereoisomer are available.⁴ When the structural assignment of NMR spectra is not possible the theoretical calculation is a method of choice as we showed in the case of chiral sulfoxides.⁵ The same approach was successfully applied also for the *N*-oxides of tertiary amines and some nitrogen containing heterocycles.^{6,7}

The 'conformationally locked' *tert*-butylcyclohexanes and their substituted derivatives were used in many stereochemical studies.⁸ In this paper we characterize the series of the 4-*tert*-butyl six-membered saturated heterocycles (N, P, S, Se) by ¹H and ¹³C NMR and study the effect of their oxidation on ¹³C and ¹H chemical shifts in well-defined geometries of the corresponding isomeric *N*-oxides, phosphinoxides, sulfoxides, and selenoxides. Different quantum chemical methods of chemical shift calculation were tested to reproduce the experimental NMR data.

2. Results and discussion

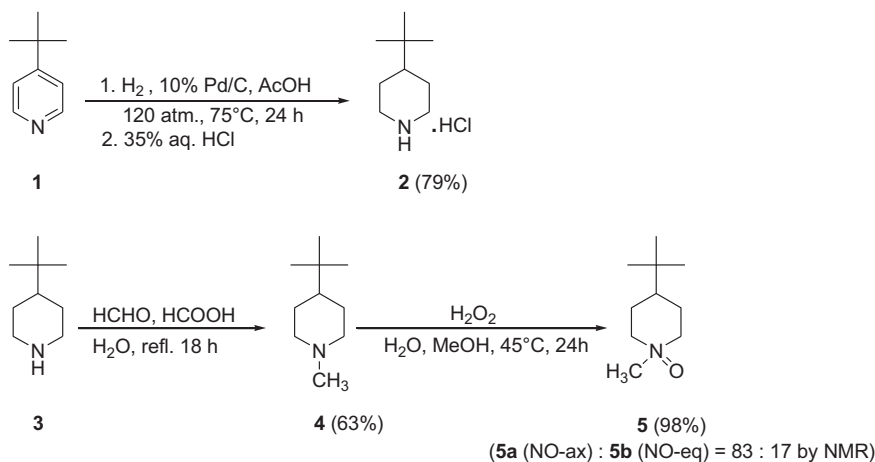
2.1. 'Classical' synthetic preparations

For all of the syntheses, 4-*tert*-butylpyridine (1) was used as a convenient starting material. At first, we attempted its hydrogenation at 80 °C and 5 MPa over PtO₂ in EtOH–CHCl₃ solution⁹ but

* Corresponding author. Tel.: +420 220 183 497; fax: +420 220 183 123; e-mail address: budesinsky@uochb.cas.cz (M. Buděšínský).

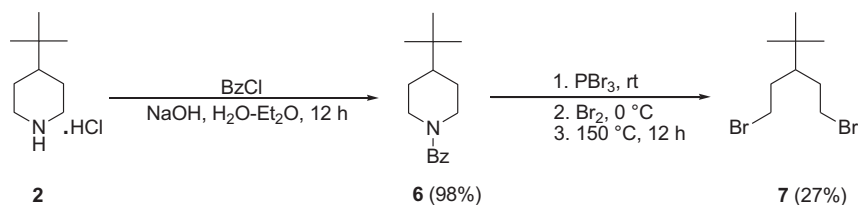
this method led repeatedly to just a partial conversion to the desired 4-*tert*-butylpiperidine (**3**), possibly due to enclosing of the catalyst into emerging hydrochloride crystals in a highly concentrated solution. In contrast, hydrogenation by a slightly modified alternative procedure¹⁰ at 75 °C and 12 MPa over 10% Pd/C in acetic acid proceeded smoothly, giving compound **3** in high yield (isolated as hydrochloride **2**).

Its *N*-methyl derivative, **4**, was prepared by Eschweiler–Clarke reaction (reductive methylation by formaldehyde–formic acid mixture);¹¹ oxidation of **4** by hydrogen peroxide afforded the corresponding *N*-oxide¹² as an *N*-epimeric mixture (**5a:5b**=83:17 by NMR) (Scheme 1).



Scheme 1.

The key intermediate for the synthesis of phosphorus, sulfur and selenium heterocycles, 4-*tert*-butyl-1,5-dibromopentane (**7**), was prepared from *N*-benzoyl derivative **6**^{13,14} by the von Braun degradation route; however, in an effort to avoid the unpleasant vacuum distillation of the aggressive reaction mixture during the work-up procedure, we diluted the mixture with acetonitrile and extracted the crude product with hexane. This method provided **7** in a yield comparable to the yield obtained by the distillation approach (Scheme 2).



Scheme 2.

The synthesis of the phosphinane ring was accomplished from dibromide **7** and in situ generated bistrimethylsilyl phosphonate (BTSP)¹⁵ in yields 42–49%. Subsequent treatment of the phosphinic acid **8**¹⁶ with oxalyl chloride afforded chloride **9**¹⁶ (as epimeric mixture **9a:9b**=80:20 by NMR), which, after reaction with methylmagnesium bromide, gave phosphinoyl **10**¹⁷ (as *P*-epimeric mixture **10a:10b**=87:13 by NMR). The desired phosphine **11** (mentioned in the work by Marsi et al.¹⁷ but without sufficient experimental data) was eventually obtained by reduction of **10** by phenyl silane as a *P*-epimeric mixture **11a:11b**=83:17 by NMR (Scheme 3).

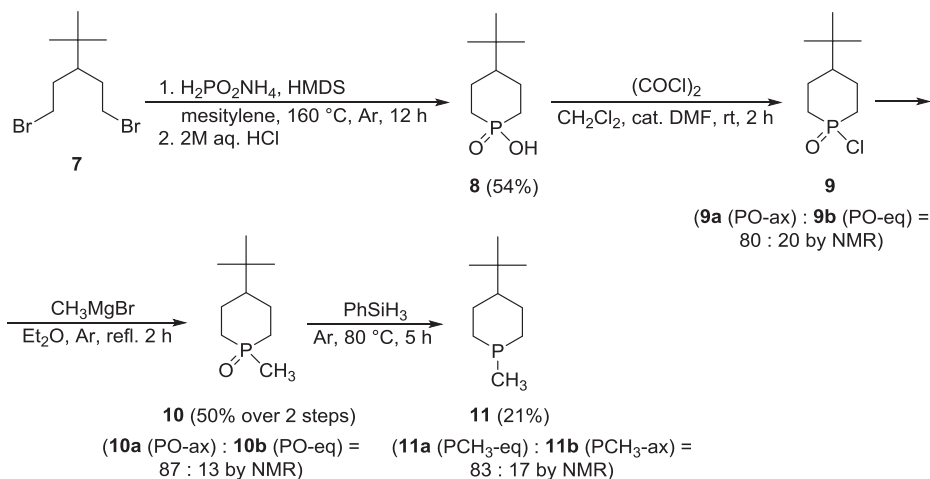
4-*tert*-Butylthiane **12**¹³ was synthesized from dibromide **7** by treatment with sodium sulfide at elevated temperature along with a small amount of 5-*tert*-butyl-1,2-dithiepane **13** by-product. Oxidation of sulfide **12** by hydrogen peroxide¹³ afforded, after two days at room temperature, the expected sulfoxide **14** (as a *S*-epimeric mixture **14a+14b**=62:33 by NMR) and a small amount (5%) of sulfone **15** (Scheme 4).

The selenium analogue, 4-*tert*-butylselenane **16**, was prepared from dibromide **7** by reaction with in situ generated hydrogenselenide upon prolonged heating. While we were not able to reproduce the method of Szczepina et al.,¹⁸ modification of the procedure by Braverman et al.¹⁹ gave **16** in high yield. In an effort to

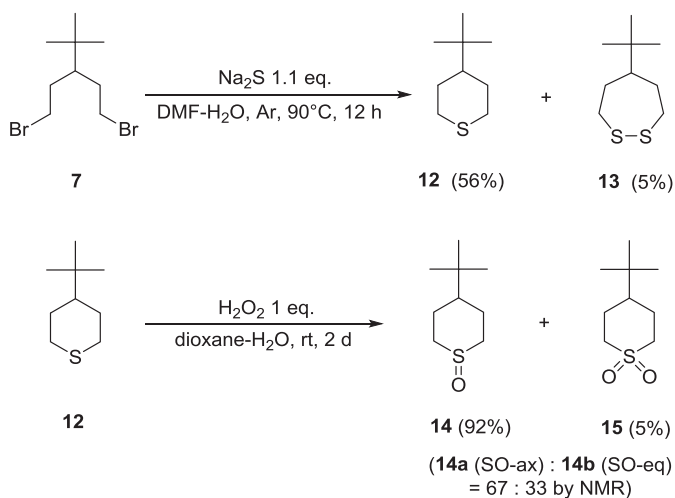
obtain the corresponding selenoxide, we attempted its oxidation by sodium periodate. However, purification of the product via HPLC with mobile phase containing trifluoroacetic acid afforded hydroxyselenonium trifluoroacetate **17**. Similarly, direct extraction of the oxidized compound from the reaction mixture led to the isolation of periodate **18**. Isolation and characterization (X-ray, NMR) of such type of hydroxyselenonium salts (alkyl sulfonates) was first claimed by Procter et al.²⁰ in 1994. In 1967, Paetzold²¹ described isolation (and characterization by IR and Raman spec-

troscopy) of similar nitrates and perchlorates. Selenoxide **19** (as *Se*-epimeric mixture **19a+19b**=82:18 by NMR) was eventually obtained by careful oxidation of **16** with hydrogen peroxide. Finally, oxidation of **16** by either KMnO₄²² or excess hydrogen peroxide at room temperature and neutral conditions gave selenone **20** (Scheme 5).

The obtained single crystals of selenoxide **19a** and selenone **20** were used for X-ray structure analysis. The selenoxide **19a** showed two slightly different molecules in the unit cell (*Z'*=2) while selenone **20** gave only one molecule (see ORTEP views in Fig. 1).



Scheme 3.



Scheme 4.

2.2. In situ oxidations with MCPBA in NMR tube

In our previous paper, we have described a simple way for the oxidation of chloroform solutions of sulfides and tertiary amines to sulfoxides and *N*-oxides by in situ reaction with *meta*-chloroperoxybenzoic acid (MCPBA) in an NMR tube.^{5–7} We have used the same method in this paper for the oxidation of 4-*tert*-butyl-tetrahydro-2*H*-thiopyran (**12**) and 4-*tert*-butyl-1-methylpiperidine (**4**) and successfully applied also for oxidation of 4-*tert*-butyl-1-methylphosphinane (**11a,b**) and 4-*tert*-butyl-tetrahydro-2*H*-selenopyran (**16**). The stepwise addition of MCPBA leads first to the epimeric mixtures of the corresponding *N*, *S*, *P* or *Se*-oxides. In the case of *S*- and *Se*-oxides the final product obtained with excess of MCPBA is the corresponding sulfone **15** and selenone **20**. The reaction course and relative amounts of the products and MCPBA (or *meta*-chlorobenzoic acid, MCBA) can be easily followed in ^1H and ^{13}C NMR spectra of the reaction mixture.

There is one drawback of this method. The presence of MCPBA/MCBA can produce a partial protonation of the oxygen atom of the substrate (depending on the substrate basicity and concentration of the acid) and to fast exchange between protonated and non-protonated species. As a result the observed chemical shifts are somewhat different from those found for acid-free oxidized products obtained by the classical synthesis and isolation. Chemical shift

differences are rather small for phosphinoyl, sulfoxides and selenoxides but somewhat larger for *N*-oxides (see detail discussion in our previous paper⁷). The comparison of the NMR data obtained by the classical oxidation with H_2O_2 and in situ reaction with MCPBA is shown in Table 1. To eliminate a possible source of inaccuracies we have exclusively used experimental data obtained for isolated products from the classical oxidation for comparison with the calculated chemical shifts. For the same reason, we have not used the literature data accessible for some of the studied compounds (referred to in Experimental part).

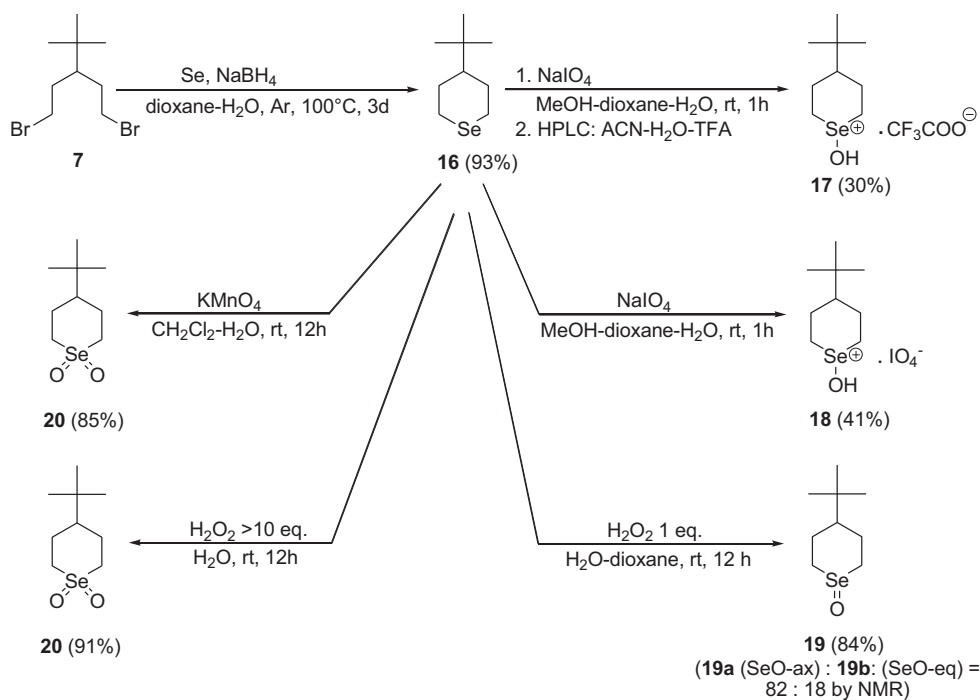
2.3. Experimental NMR data of six-membered heterocycles (N, P, S, Se) and their oxidation products

The ^1H and ^{13}C NMR data were collected for the six-membered heterocycles (*N*, *P*, *S*, *Se*) and their oxidation products. In the case of nitrogen-, phosphorus- and selenium-containing heterocycles we have collected also ^{15}N , ^{31}P and ^{77}Se chemical shifts, respectively. Experimental NMR data are presented in Figs. 2–8. The NMR spectra of ^{17}O in all oxidized forms and ^{33}S in sulfur containing heterocycles were not measured since they have very limited practical application due to low natural abundance and very broad lines (spin 5/2 and 3/2, resp.).

The ranges of NMR shifts are influenced by different electronegativity of the introduced heteroatoms (Pauling electronegativities: $\text{N}=3.04 > \text{S}=2.58 \sim \text{Se}=2.55 > \text{P}=2.19$). The largest range of ^1H and ^{13}C chemical shift was observed for the *N*-heterocycles, smaller for the *S*- and *Se*-heterocycles and the smallest for the *P*-heterocycles. The range of the observed chemical shifts has an effect on the reliability of the NMR determination of configuration on the heteroatom in the oxidized forms.

2.4. Geometry of studied heterocycles and their oxidized products

The geometries of the studied molecules were optimized in vacuum using different quantum chemical methods. The selected bond lengths, bond angles and torsion angles calculated using DFT B3LYP/6-31G* method together with calculated data for *tert*-butylcyclohexane **21** and 4-*tert*-butyl-tetrahydropyran **22** and X-ray data for selenoxide **19a** and selenone **20** are summarized in Table 2. The replacement of carbon atom with nitrogen and oxygen leads to small shortening of the C-X bond but other heteroatoms (*P*, *S*, *Se*) induce significant prolongation of this bond from $\sim 1.83 \text{ \AA}$ (*S*) to $\sim 1.87 \text{ \AA}$ (*P*) up to $\sim 1.97 \text{ \AA}$ (*Se*). This is accompanied by



Scheme 5.

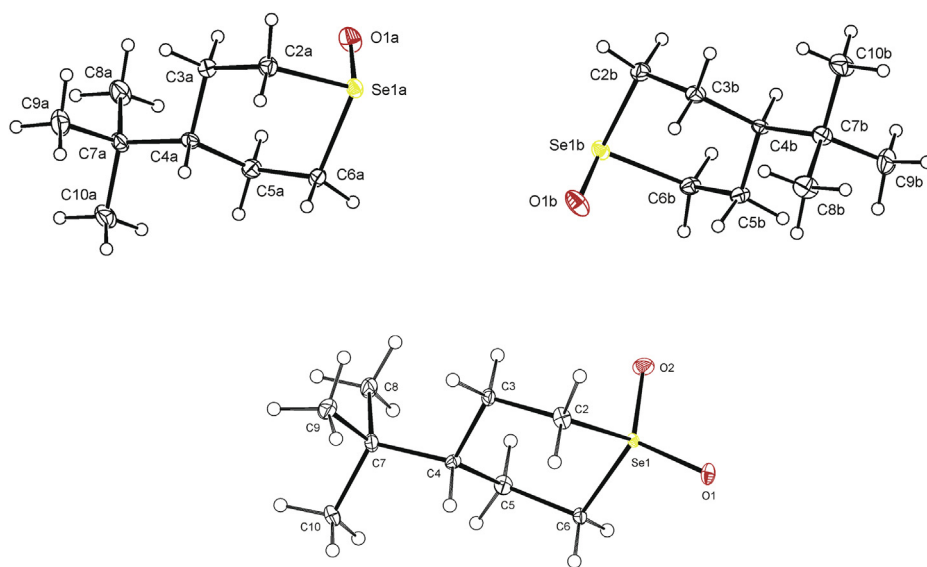


Fig. 1. View on two symmetrically independent molecules of **19a** (top) and a single molecule **20** (bottom). Displacement ellipsoids are drawn on 30% probability level.

a remarkable decrease of the bond angle C2-X-C6 and some changes of endocyclic torsion angles in P-, S- and Se-heterocycles. The oxidation of the heteroatom has only a small effect on the bond length C-X. The bond lengths X-O increase from X=N (1.36 Å), over X=P or X=S (~1.50 Å) up to X=Se (~1.65 Å). The comparison of the calculated geometry parameters and X-ray data for selenoxide **19a** and selenone **20** are in very good agreement. It shows that the theoretical calculations can provide realistic geometry parameters of the studied molecules.

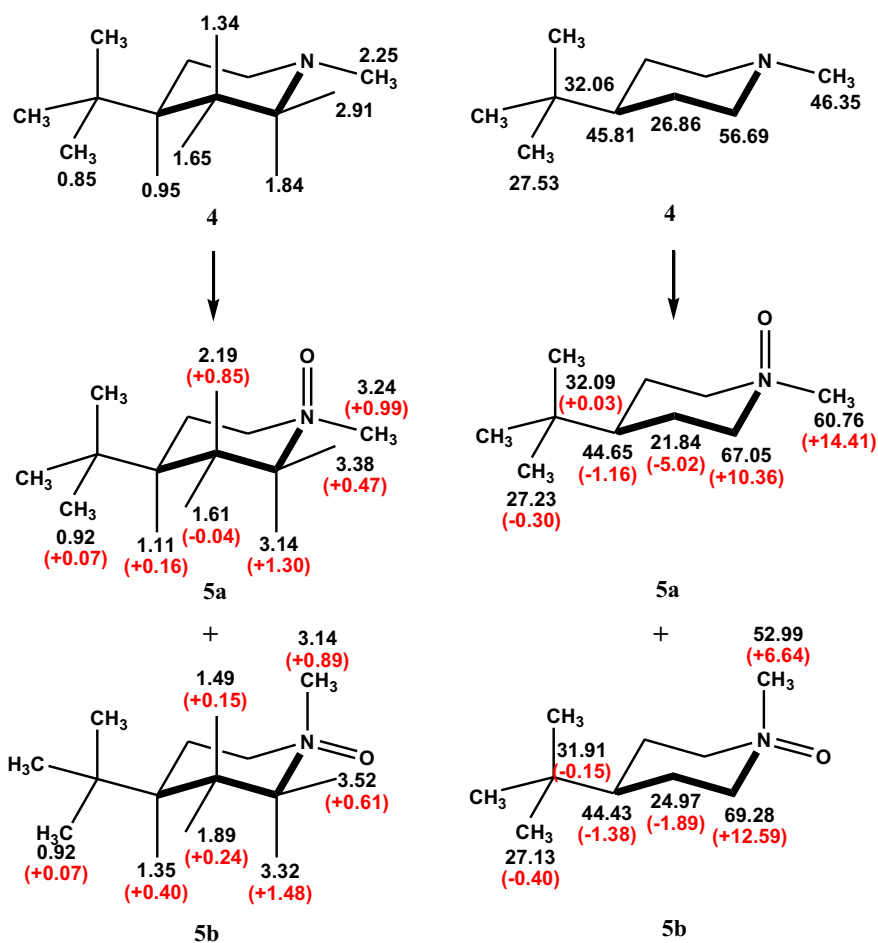
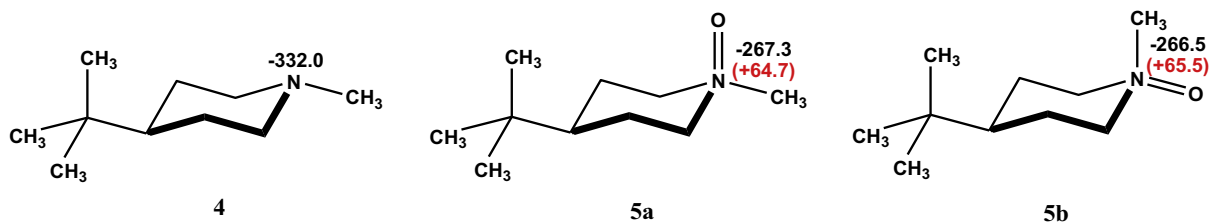
2.5. Comparison of the observed and calculated chemical shifts

The ^{13}C and ^1H NMR shifts calculated in vacuum with DFT employing different functionals and HF and MP2 methods are

shown in Table 3. Mean absolute error (MAE) values are given for ^{13}C and ^1H shifts for each group of the studied heterocycles (N, P, S, Se) and given method of calculation. For two methods of calculation (1) OPT and NMR, B3LYP/6-31G*/B3LYP/6-31G*, and (2) OPT and NMR, B3LYP/6-311G**/B3LYP/6-311G** we have checked the effect of introducing an implicit solvent (PCM model, solvent=chloroform) into the calculation. The calculations were done for all four combinations: (a) both OPT and NMR in vacuum, (b) OPT in chloroform and NMR in vacuum, (c) OPT in vacuum and NMR in chloroform, (d) both OPT and NMR in chloroform. For ^{13}C chemical shifts the best results were obtained for combination OPT in chloroform and NMR in vacuum while for ^1H chemical shifts it was the combination with both OPT and NMR in chloroform. However, the differences in the results obtained with the four combinations are in general rather small (see data in Table 3).

Table 1Comparison of NMR data of isolated products and those from in situ oxidation with MCPBA in NMR tube ($\Delta\delta = \delta(\text{in situ oxid.}) - \delta(\text{isol. oxid. prod.})$)

	N=O ax	N=O eq	P=O ax	P=O eq	S=O ax	S=O eq	SO ₂	Se=O ax	Se=O eq	SeO ₂
¹³ C/ppm										
X-CH ₃	-2.47	-1.85	-0.26	-0.20	—	—	—	—	—	—
C-2,6	-0.86	-1.98	-0.24	-0.33	-0.37	-0.74	-0.01	-0.60	-1.48	+0.12
C-3,5	-0.20	-0.72	-0.01	-0.08	+0.09	+0.02	-0.01	+0.29	-0.04	+0.01
C-4	-0.62	-0.71	-0.08	-0.11	-0.17	-0.19	-0.03	-0.36	-0.31	+0.20
>C<	-0.02	+0.16	+0.03	+0.04	+0.02	+0.01	0.00	+0.11	0.00	0.00
(CH ₃) ₃	-0.15	-0.13	0.00	0.00	-0.01	+0.01	+0.01	-0.04	-0.18	-0.06
¹ H/ppm										
X-CH ₃	+0.36	+0.31	+0.07	+0.06	—	—	—	—	—	—
H-2ax,6ax	-0.03	+0.38	+0.02	+0.11	0.00	+0.16	+0.01	+0.08	+0.32	+0.12
H-2eq,6eq	+0.66	+0.40	+0.11	+0.07	+0.09	+0.07	+0.02	+0.28	+0.16	+0.08
H-3ax,5ax	-0.03	+0.08	+0.01	+0.02	+0.01	+0.01	0.00	+0.01	+0.01	0.00
H-3eq,5eq	+0.11	+0.07	+0.02	+0.01	+0.03	+0.02	0.00	+0.05	+0.03	0.00
H-4	+0.07	+0.09	+0.01	+0.03	+0.01	+0.03	0.00	+0.03	+0.08	+0.04
(CH ₃) ₃	-0.01	0.00	0.00	0.00	0.00	0.00	0.00	0.00	0.00	-0.01

**Fig. 2.** The ¹H (left) and ¹³C (right) chemical shifts (in black) of 4-*tert*-butyl-1-methylpiperidine and the products obtained by its oxidation with H₂O₂. The chemical shift changes ($\Delta\delta$ values) induced by oxidation are given in brackets (in red).**Fig. 3.** The ¹⁵N chemical shifts of 4-*tert*-butyl-1-methylpiperidine and the products obtained by its oxidation with H₂O₂. The chemical shift changes ($\Delta\delta$ values) induced by oxidation are given in brackets (in red).

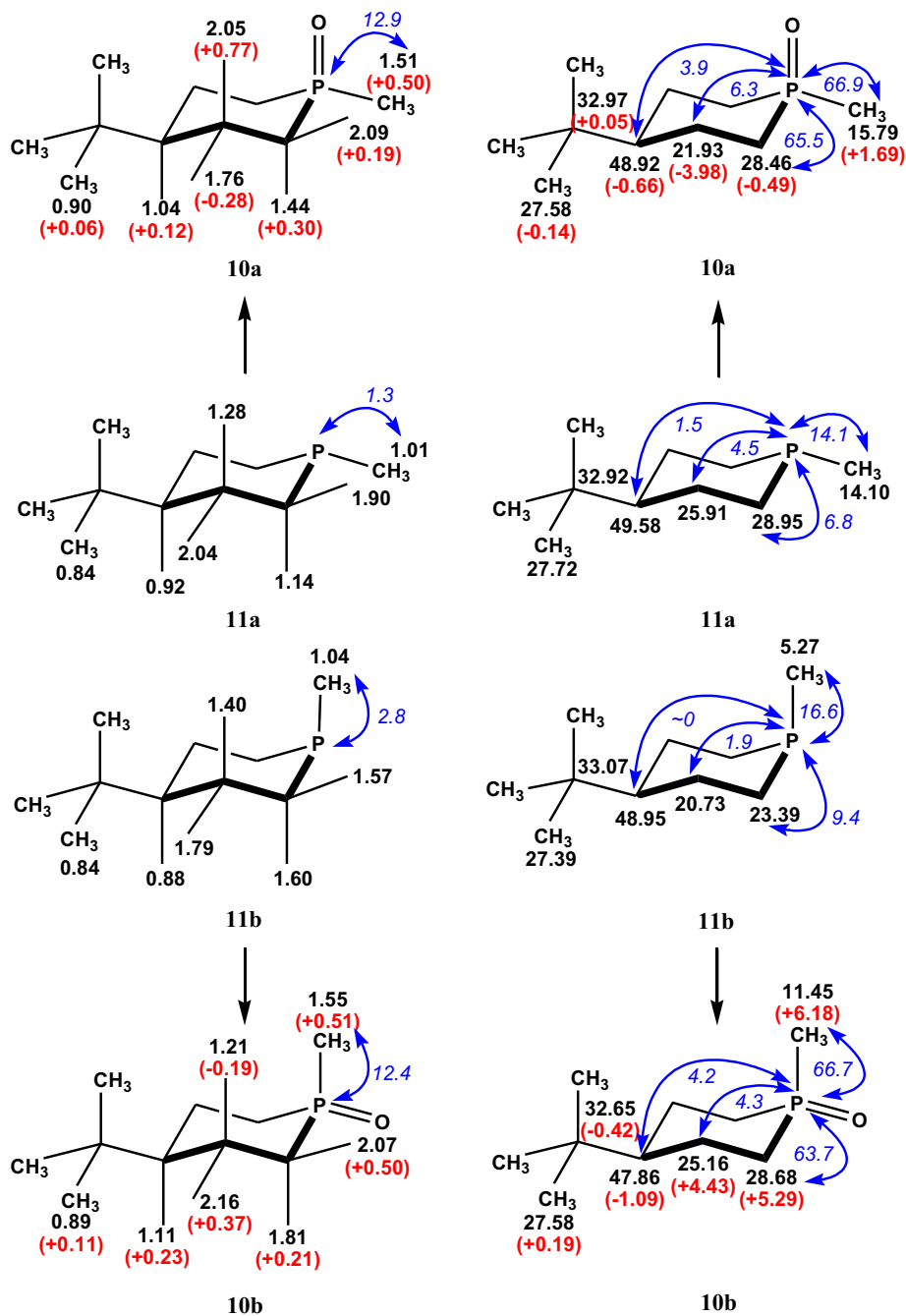


Fig. 4. The ^1H (left) and ^{13}C (right) chemical shifts (black) of 4-tert-butyl-1-methylphosphinane and the products obtained by its oxidation with H_2O_2 . The chemical shift changes ($\Delta\delta$ values) induced by oxidation are given in brackets (red) and coupling constants $J(\text{P,C})$ and $J(\text{P,CH}_3)$ are shown with arrows in blue. Additional $J(\text{P,H})$ were not determined due to complex multiplet patterns of the endocyclic hydrogens.

As we have shown in our previous studies^{5–7} the useful parameters for the determination of the configuration in sulfoxides and *N*-oxides are the so-called oxidation induced shifts, i.e., differences between the chemical shift of the oxidized form and its corresponding precursor ($\Delta\delta$). Therefore, we have also calculated oxidation shifts from the calculated NMR chemical shifts and compared them with the experimental ones. The differences between the calculated and experimental $\Delta\delta$ values (MAE_{oxid}) for each group of the studied heterocycles (N, P, S, Se) and given method of calculation are summarized in Table 4. Introduction of an implicit solvent (PCM model, solvent=chloroform) into the calculation provides slightly better values of the oxidation induced ^{13}C and ^1H

shifts for the combination OPT and NMR both in chloroform (see data in Table 4).

As can be seen from Tables 3 and 4 neither of the methods gives the best results for both ^1H and ^{13}C chemical shifts of all studied heterocycles. There is also not a very clear improvement when going to the higher level of theory. Since there are mostly not substantial differences in MAE values obtained by different methods a practical choice seems to be a simple method OPT and NMR using DFT B3LYP/6-31G*, in accordance with the conclusion of Hommes and Clark.²³

A correlation of the experimental and calculated ^{13}C and ^1H chemical shifts (OPT and NMR using DFT B3LYP/6-31G*) for all

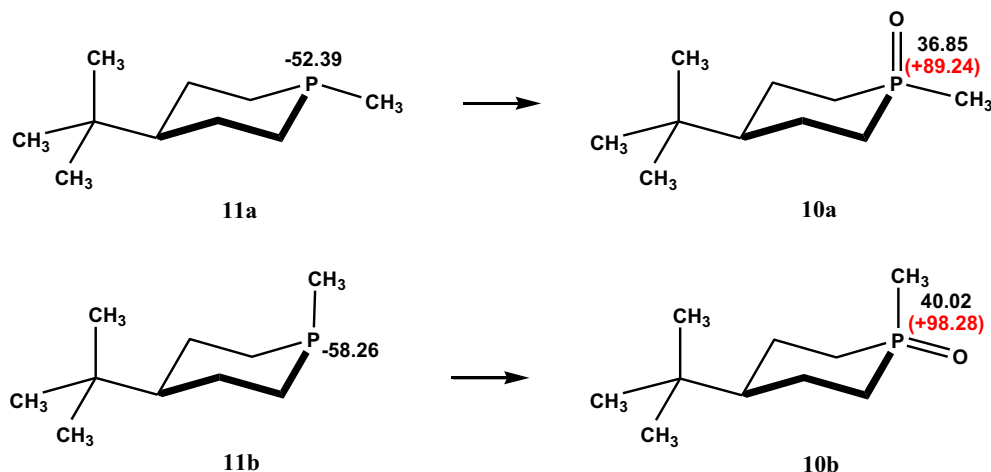


Fig. 5. The ^{31}P chemical shifts of 4-*tert*-butyl-1-methylphosphinane and the products obtained by its oxidation with H_2O_2 . The chemical shift changes ($\Delta\delta$ values) induced by oxidation are given in brackets (red).

studied heterocycles is shown in Fig. 9. Carbon-13 chemical shifts give significantly better linear correlation than hydrogens.

2.6. The use of NMR chemical shifts for the determination of the configuration at the heteroatom

A comparison of the observed and calculated (GIAO, B3LYP/6-31G*) ^1H and ^{13}C chemical shifts and oxidation induced shifts is given in Table 5. The data for ^1H and ^{13}C of *tert*-butyl group that are far from the heteroatom and, therefore, only very slightly influenced by the oxidation, are not shown. The comparison of the experimental and calculated relative positions of the signals of O(ax) and O(eq) stereoisomer for the pairs of NO, PO SO and SeO compounds in Table 5 shows, in general, a good agreement. Only few exceptions are the cases with very similar chemical shift values for both isomers. There is also a clear analogy in behavior of the NO, PO, SO, and SeO heterocycles. Carbon atoms in the α - and β -positions to the heteroatom have higher δ -values (and oxidation induced shifts) in O(eq) isomers while the opposite situation (lower δ -values in O(ax) isomers) is seen for γ - and X- CH_3 carbon atoms. Smaller differences but similar regularities can be found for the behavior of the hydrogen atoms. Both H-ax and H-eq on C α , H-eq on C β and H-ax on C γ have higher δ -values (and oxidation induced shifts) in O(eq) isomers while the opposite (lower δ -values in O(ax) isomers) is true for H-ax on C β - and X- CH_3 . General rules for relations between ^{13}C and ^1H chemical shifts of carbon and hydrogen atoms in different positions of O(ax) and O(eq) stereoisomers are graphically shown in Fig. 10.

Chemical shifts of heteroatoms— ^{15}N , ^{31}P , and ^{77}Se —can easily distinguish the oxidized forms from their precursors (see data in Figs. 3, 5, and 8). However, the difference between O(ax)- and O(eq)-isomers is close to zero in ^{15}N , somewhat larger in ^{31}P and rather large in ^{77}Se NMR chemical shifts, always showing higher positive δ -value for the O(eq)-isomer (see Figs. 3, 5, and 8).

3. Conclusions

We can conclude that quantum chemical calculation of carbon-13 chemical shifts and/or oxidation induced shifts can be used for the configuration determination at the heteroatom in N-oxides, P-oxides, S-oxides, and Se-oxides. Satisfactory agreement between calculated and observed shifts can be obtained already with a simple and fast DFT B3LYP/6-31G* method. The proton chemical shifts and/or oxidation induced shifts must be used more carefully

due to much smaller chemical shift differences (namely in the case of P-oxides) and their sensitivity to solvent. The agreement between calculated and observed ^1H chemical shifts can be somewhat improved using B3LYP/6-311G** method with implicit solvent (PCM model) in both geometry optimization and chemical shift calculation.

4. Experimental

4.1. General chemistry

Unless otherwise stated, reagents and solvents used in this study were obtained from commercial suppliers (Sigma–Aldrich, Fluka, Merck) and used without purification. The solvents were evaporated at 55 °C and 2 kPa, and the products were dried over phosphorus pentoxide at rt and 13 Pa. TLC on silica gel coated aluminum plates (Fluka) was performed in the following systems (v/v): chloroform–ethanol 9:1 (C1); chloroform–ethanol 19:1 (C2); ethyl acetate–acetone–ethanol–water 4:1:1:1 (H1); ethyl acetate–acetone–ethanol–water 6:1:1:0.5 (H3); 50% ethyl acetate–toluene (T1); 20% EtOAc–toluene (T2); 5% EtOAc–toluene (T3), hexane–toluene 2:1 (HT). The compounds were visualized by exposure to UV light at 254 nm, by ninhydrin spraying (dark color of amines upon heating), by 1% aq KMnO_4 spraying (yellow color of oxidizable compounds) and by spraying with a 1% ethanolic solution of 4-(4-nitrobenzyl)pyridine followed by heating and treating with gaseous ammonia (blue color of esters and alkylating compounds). Flash chromatography purifications were carried out on silica gel (40–63 μm , Fluka). Preparative RP-HPLC chromatography of the target compounds was carried out on a C18 Luna column (Phenomenex, 250 x 21.2 mm, 10 μm) at a flow rate 9 ml/min. Solvent A: 0.1% TFA in H_2O . Solvent B: 80% CH_3CN , 0.1% TFA, H_2O . The following gradient was used: $t=0$ min (10% B), $t=30$ min (60% B), $t=31$ min (10% B). HRMS spectra were obtained on a FTMS mass spectrometer LTQ-orbitrap XL (Thermo Fisher, Bremen, Germany) in electrospray ionization mode or in case HRMS (EI) on GCT Premier (Waters). Purity of target compounds was confirmed by elemental analysis (C, H, N, S, Se, P, F, Br, I) agreeing with calculated values within 0.4%. Density of liquid compounds was measured at 23 °C.

4.2. NMR experiments

The ^1H and ^{13}C NMR spectra were measured on a Bruker AVANCE 600 instrument (^1H at 600.13 MHz and the ^{13}C at

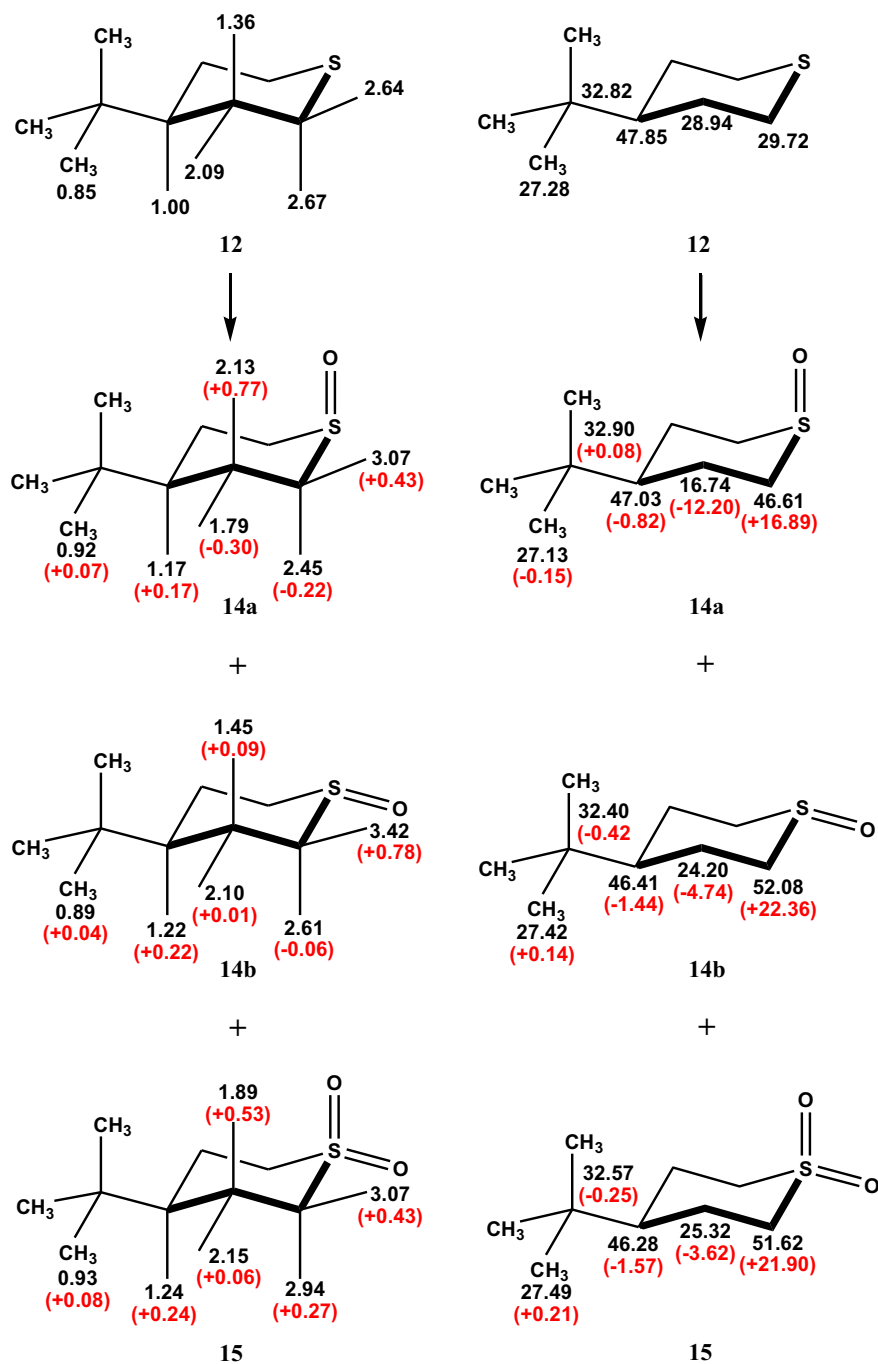


Fig. 6. The 1H (left) and ^{13}C (right) chemical shifts (black) of 4-tert-butyl-tetrahydro-2H-thiopyran and of the products obtained by its oxidation with H_2O_2 . The oxidation induced chemical shift changes ($\Delta\delta$ values) are given in brackets (red).

150.9 MHz frequency using a 5 mm TXI cryo-probe) in $CDCl_3$, $DMSO-d_6$, CD_3OD or D_2O solution at 300 K. About 5–10 mg of the sample in 0.6 ml of $CDCl_3$ was used for heterocycles and their oxidized product. The chemical shifts are given in δ -scale (with the 1H shifts referenced to TMS and the ^{13}C shifts referenced to $CDCl_3$ using $\delta(CDCl_3)$ 77.00 ppm). The typical experimental conditions for the 1H NMR spectra were sixteen scans, with a spectral width of 6 kHz and an acquisition time of 5 s, yielding 60 K data points. The FIDs were zero-filled to 128 K data points. 2D-homonuclear (H,H-COSY and H,H-ROESY) and 2D-heteronuclear (H,C-HSQC and H,C-HMBC) experiments were performed for the structural assignments of signals (with standard 2D-NMR pulse sequences of the

Bruker software being used). The ^{15}N chemical shifts were obtained from 2D-H,N-HMBC spectra and referenced to CH_3NO_2 ($\delta(^{15}N)$ = 0 ppm), added to the $CDCl_3$ solution as an internal reference. The ^{31}P and ^{77}Se NMR spectra were recorded on a Bruker AVANCE 500 (^{31}P at 202.3 MHz and ^{77}Se at 95.3 MHz) using H_3PO_4 ($\delta(^{31}P)$ = 0 ppm) and dimethylselenene ($\delta(^{77}Se)$ =0 ppm) as external standards.

4.3. Theoretical calculation of molecular geometry and NMR chemical shifts

The geometry optimizations and shielding constants of carbon and hydrogen atoms in six-membered heterocycles (N, P, S, Se)—4-

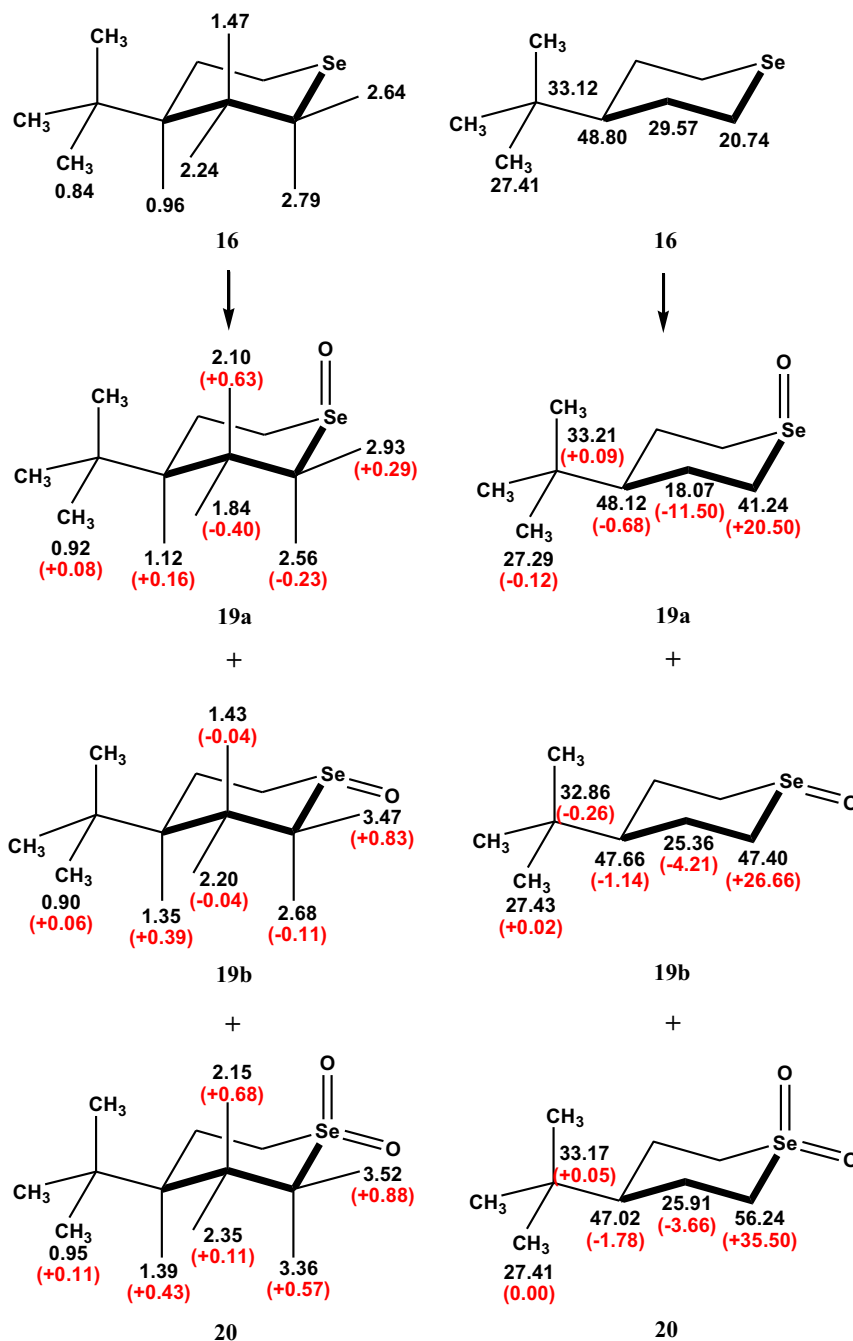


Fig. 7. The ^1H (left) and ^{13}C (right) chemical shifts (black) of 4-*tert*-butyl-tetrahydro-2*H*-selenopyran and the products obtained by its oxidation with H_2O_2 . The oxidation induced chemical shift changes ($\Delta\delta$ values) are given in brackets (red).

tert-butyl-1-methylpiperidine, 4-*tert*-butyl-1-methylphosphinane, 4-*tert*-butyl-tetrahydro-2*H*-thiopyran, and 4-*tert*-butyl-tetrahydro-2*H*-selenopyran and their oxidation products were calculated by quantum chemical methods at different levels of theory using the Gaussian 03 software package.²⁴ DFT, HF, and MP2 methods in vacuum (see Table 2) were used to optimize molecular geometry of the studied compounds. The nuclear magnetic shielding constants were calculated for the geometry-optimized structures using gauge-including atomic orbitals (GIAO) with DFT, HF and MP2 methods with different basis sets (see Table 2). Shielding constants were converted to chemical shifts using shielding constants of tetramethylsilane, calculated at the same level of theory. The calculated chemical shifts were then compared with the experimental

values and mean average errors (MAE) were calculated. For two selected DFT methods (B3LYP-6-31G* and B3LYP-6-311G**) the geometry optimization and NMR shielding constants were also calculated in chloroform using the PCM model.

4.4. The X-ray structure analysis of selenoxide 19a and selenone 20

Single-crystal X-ray diffraction data for **19a** and **20** were obtained from Nonius KappaCCD diffractometer equipped with Bruker ApexII detector by monochromatized $\text{MoK}\alpha$ radiation ($\lambda=0.71073$ Å) at 150(2) K. The structures were solved by direct methods (SHELXS, 2008) and refined by full-matrix least squares

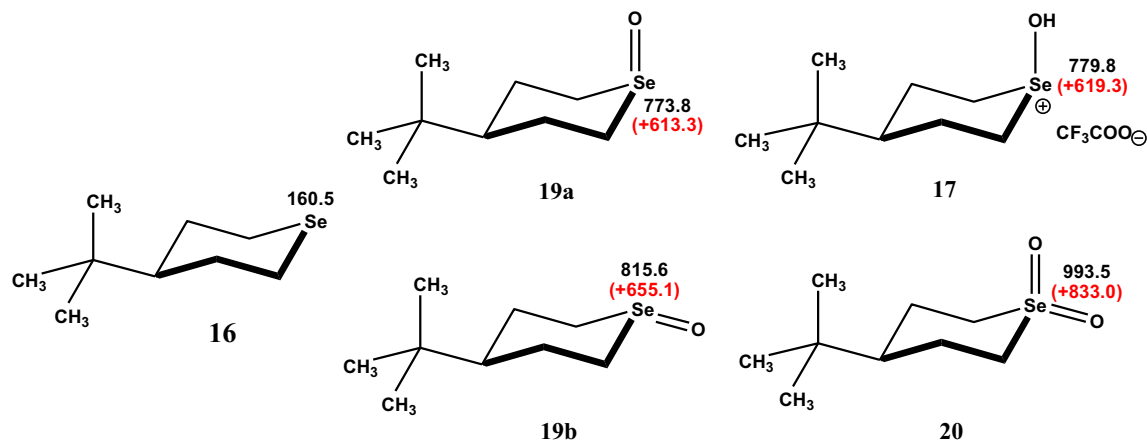
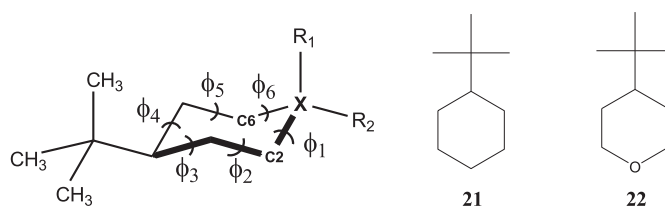


Fig. 8. The ^{77}Se chemical shifts (black) of 4-*tert*-butyl-tetrahydro-2H-selenopyran and the products obtained by its oxidation. The oxidation induced chemical shift changes ($\Delta\delta$ values) are given in brackets (red).

Table 2

Calculated geometry parameters of the studied heterocycles (DFT B3LYP/6-31G^{*}). The X-ray data for **19a** and **20** are given in italics



Comp.	X	R ₁	R ₂	Bond lengths [Å]			Bond angles [deg]			Torsion angles [deg]		
				d(C2–X)	d(CH ₃ –X)	d(X–O)	C2–X–C6	C2–X–R ₁	C2–X–R ₂	ϕ_1^a	ϕ_2^a	ϕ_3^a
21	C	H	H	1.534	—	—	110.8	109.3	110.5	–54.2	56.0	–55.5
22	O	—	—	1.420	—	—	111.4	—	—	–59.7	56.9	–52.2
4	N	—	Me	1.460	1.453	—	111.0	—	111.8	–58.9	57.3	–53.6
5a	N	O	Me	1.519	1.497	1.359	108.2	110.3	109.5	–61.1	59.5	–54.6
5b	N	Me	O	1.515	1.501	1.358	108.1	110.9	109.4	–52.3	55.7	–53.5
11a	P	—	Me	1.872	1.867	—	95.5	—	100.7	–57.6	64.3	–60.2
11b	P	Me	—	1.875	1.871	—	97.6	101.3	—	–41.7	57.2	–63.4
10a	P	O	Me	1.837	1.834	1.504	100.2	114.4	106.2	–53.3	61.6	–62.6
10b	P	Me	O	1.837	1.836	1.503	101.2	105.6	115.0	–43.0	56.7	–63.4
12	S	—	—	1.834	—	—	97.1	—	—	–52.8	62.0	–60.6
14a	S	O	—	1.850	—	1.519	94.0	106.8	—	–58.5	65.4	–59.5
14b	S	—	O	1.844	—	1.514	94.0	—	107.9	–58.0	65.0	–59.0
15	S	O	O	1.815	—	1.474	100.1	107.8	109.3	–53.0	61.2	–61.4
16	Se	—	—	1.971	—	—	93.2	—	—	–53.6	63.8	–62.0
19a	Se	O	—	1.992	—	1.674	91.3	103.1	—	–58.9	67.4	–62.6
mol.1				1.950	—	1.673	90.9	102.9	—	–58.0	67.1	–61.8
mol.2				1.949	—	1.673	93.4	102.7	—	–52.5	65.0	–65.0
19b	Se	—	O	1.987	—	1.669	90.9	—	103.7	–55.4	65.6	–61.8
20	Se	O	O	1.956	—	1.638	97.3	106.8	110.9	–54.6	63.6	–64.2
				1.906	—	1.632	99.4	109.2	110.2	–54.0	63.0	–64.2

^a Torsion angles: $\phi_6 = -\phi_1$; $\phi_5 = -\phi_2$; $\phi_4 = -\phi_3$.

based on F^2 (SHELXL97). The hydrogen atoms were fixed into idealized positions (riding model) and assigned temperature factors $H_{\text{iso}}(\text{H}) = 1.2 U_{\text{eq}}(\text{pivot atom})$.

Crystal data for **19a**: $2(\text{C}_9\text{H}_{18}\text{OSe}) \cdot \text{H}_2\text{O}$, $M = 460.40$, Triclinic, $P-1$ (No 2), $a = 6.1387(4)$ Å, $b = 10.4161(6)$ Å, $c = 16.6555(10)$ Å, $\alpha = 81.655(2)^\circ$, $\beta = 88.992(2)^\circ$, $\gamma = 87.294(2)^\circ$, $V = 1052.46(11)$ Å³, $Z = 2$, $D_x = 1.453$ Mg m⁻³, colorless crystal of dimensions $0.48 \times 0.16 \times 0.09$ mm, numerical absorption correction ($\mu = 3.53$ mm⁻¹) $T_{\text{min}} = 0.283$, $T_{\text{max}} = 0.738$; a total of 12,753 measured reflections ($\theta_{\text{max}} = 27.5^\circ$), from which 4783 were unique ($R_{\text{int}} = 0.039$) and 3384 observed according to the $I > 2\sigma(I)$ criterion. The refinement converged ($\Delta/\sigma_{\text{max}} < 0.001$) to $R = 0.036$ for observed reflections and $wR(F^2) = 0.073$, $\text{GOF} = 1.01$ for 224 parameters and all 4783 reflections. The final difference map displayed no peaks of chemical significance ($\Delta\rho_{\text{max}} = 0.53$, $\Delta\rho_{\text{min}} = -0.60$ e Å⁻³).

The unit cell contains two symmetrically independent molecules of selenoxide differing in their intermolecular interactions. Molecules B are forming O⋯H–O hydrogen bonds with disordered water molecule, while molecule A interacts by weak O⋯H–C hydrogen bonds. However, the intramolecular parameters of both molecules are very close to each other (see Table 2). Crystal data for **20**: $\text{C}_9\text{H}_{17}\text{O}_2\text{Se}$, $M = 236.19$, Triclinic, $P-1$ (No 2), $a = 5.9623(11)$ Å, $b = 6.1295(9)$ Å, $c = 15.176(3)$ Å, $\alpha = 95.358(7)^\circ$, $\beta = 93.662(8)^\circ$, $\gamma = 111.912(5)^\circ$, $V = 509.38(16)$ Å³, $Z = 2$, $D_x = 1.540$ Mg m⁻³, colorless crystal of dimensions $0.22 \times 0.21 \times 0.06$ mm, numerical absorption correction ($\mu = 3.65$ mm⁻¹) $T_{\text{min}} = 0.500$, $T_{\text{max}} = 0.811$; a total of 9206 measured reflections ($\theta_{\text{max}} = 26^\circ$), from which 1994 were unique ($R_{\text{int}} = 0.053$) and 1858 observed according to the $I > 2\sigma(I)$ criterion. The refinement converged ($\Delta/\sigma_{\text{max}} < 0.001$) to $R = 0.073$ for observed reflections and $wR(F^2) = 0.197$, $\text{GOF} = 1.18$ for 113 parameters and all

Table 3

Overview of the MAE values of chemical shifts for different calculation methods. The lowest MAE values are highlighted by yellow or green color

$$MAE = \frac{1}{n} \sum_{i=1}^n |\delta_{calc} - \delta_{exp}|$$

OPT	NMR	¹³ C [ppm]					¹ H [ppm]				
		N NO	P PO	S SO SO ₂	Se SeO SeO ₂	Average a	N NO	P PO	S SO SO ₂	Se SeO SeO ₂	Average a
B3LYP/6-31G*	B3LYP/6-31G*	1.16	1.54	1.58	1.98	1.56	0.22	0.18	0.22	0.30	0.23
B3LYP/6-31G* ^b	B3LYP/6-31G*	1.05	1.42	1.45	1.85	1.44	0.22	0.18	0.23	0.29	0.23
B3LYP/6-31G*	B3LYP/6-31G* ^b	1.33	2.02	1.83	2.18	1.84	0.20	0.18	0.18	0.23	0.20
B3LYP/6-31G* ^b	B3LYP/6-31G* ^b	1.16	1.54	1.65	2.01	1.59	0.19	0.18	0.17	0.22	0.19
B3LYP/6-31G*	OPBE/6-31G*	1.55	1.50	1.51	2.03	1.68	0.22	0.17	0.22	0.28	0.22
HF/6-31G*	HF/6-31G*	4.75	3.31	4.44	4.77	4.32	0.35	0.30	0.34	0.45	0.36
B3LYP/6-31G*	HF/6-31G*	4.07	3.07	3.49	2.10	3.18	0.31	0.26	0.32	0.32	0.30
B3LYP/6-31G*	OPBE/6-311G*	1.78	2.35	2.66	2.27	2.27	0.20	0.16	0.18	0.28	0.20
B3LYP/6-31G**	OPBE/6-31G**	1.34	1.72	1.72	2.05	1.71	0.20	0.15	0.19	0.28	0.20
B3LYP/6-31G**	B3LYP/6-31G**	1.68	1.91	2.21	2.68	2.12	0.20	0.17	0.22	0.27	0.22
B3LYP/6-311G**	B3LYP/6-311G**	4.23	4.31	5.08	5.72	4.83	0.16	0.17	0.20	0.22	0.19
B3LYP/6-311G** ^b	B3LYP/6-311G**	4.13	4.18	5.03	5.56	4.73	0.18	0.16	0.20	0.22	0.19
B3LYP/6-311G**	B3LYP/6-311G** ^b	4.59	4.49	5.38	6.14	5.15	0.14	0.14	0.12	0.14	0.13
B3LYP/6-311G** ^b	B3LYP/6-311G** ^b	4.44	4.39	5.24	6.00	5.02	0.13	0.14	0.12	0.14	0.13
B3LYP/6-31G**	B3LYP/6-31++G**	3.91	4.70	4.68	5.32	4.65	0.29	0.31	0.19	0.33	0.28
HF/6-311++G**	HF/6-311++G**	2.23	1.10	1.50	2.99	1.96	0.42	0.38	0.45	0.51	0.44
MP2/6-311++G**	HF/6-311++G**	1.65	1.04	1.37	2.71	1.69	0.42	0.30	0.36	0.41	0.37
MP2/6-311++G**	MP2/6-311++G**	3.98	3.69	4.20	4.18	4.01	0.37	0.28	0.22	0.27	0.28

^a MAE for all studied heterocycles; ^b PCM model, solvent = chloroform.

1994 reflections. The final difference map displayed no peaks of chemical significance ($\Delta\rho_{\max}=2.35$, $\Delta\rho_{\min}=-2.65$ Å⁻³). The crystal **20** was non-merohedral twin with volume ratio of two parts 0.790:0.210 (the contribution of the second part was included into the refinement [twin matrix for *hkl* indices (-1 0 0; 0 -1 0; 0.580 0.670 1)]. The twinning is probably the reason for lower precision of the structure determination.

Crystallographic data (excluding structure factors) for the structures have been deposited with the Cambridge Crystallographic Data Centre with CCDC numbers 958773 and 958774 for **19a** and **20**, respectively. Copies of the data can be obtained, free of charge, on application to Cambridge Crystallographic Data Centre, 12 Union Road, Cambridge CB2 1EZ, UK, (fax: +44-(0)1223-336033 or e-mail: deposit@ccdc.cam.ac.uk).

4.5. Preparation of the studied heterocycles

4.5.1. 4-tert-Butylpiperidine hydrochloride (2). Elemental analysis of the starting 4-tert-butylpyridine (**1**, purchased from Sigma–Aldrich) revealed sulfur content of about 0.2%. Thus, prior to hydrogenation, the commercial compound was desulfurized by conversion to hydrochloride and recrystallization from Et₂O–Me₂CO mixture. The hydrochloride was then partitioned between Et₂O and 10 M aq NaOH, the organic layer was dried over Na₂SO₄, excessive Et₂O evaporated, and the residue was distilled in vacuo to give 4-tert-butylpyridine with sulfur content lower than 0.01%, which was considered satisfactory for further processing.

To a solution of the purified 4-tert-butylpyridine (77.0 g, 0.569 mol) in acetic acid (600 mL) in a 900-mL stainless steel reactor equipped with mechanic stirrer, gas inlet, gas outlet,

a thermocouple to check the internal temperature, and external heating bath, 5 g of 10% palladium on charcoal was introduced under nitrogen atmosphere and the external temperature set to 80 °C. The reactor was pressurized with hydrogen to 12 MPa and heated upon stirring for 12 h. After cooling to room temperature, the catalyst was filtered off the reaction mixture, the acetic acid was removed in vacuo, and the residue was co-distilled with 60 mL of 35% hydrochloric acid. Crude hydrochloride was then successively co-distilled with water (100 mL) and MeOH (2×250 mL). The resulting pale-yellow crystalline mass was dissolved in MeOH (750 mL), the turbid solution was filtered and the volume was reduced to 500 mL by evaporation in vacuo at 55 °C. After addition of acetone (500 mL) and cooling to room temperature, the solution was kept at -20 °C for 12 h. The white glistening platelets were filtered off, washed with Et₂O and dried in vacuo to afford 79.32 g of hydrochloride **2**.

The filtrate was evaporated to dryness and recrystallized in a similar manner from MeOH/acetone (100/400 mL) mixture, giving 11.37 g; finally, repeating of the crystallization for the third time afforded, after 2 days at -20 °C, 2.14 g of the hydrochloride, i.e., 92.83 g (0.52 mol, 91.7%) of **2** in total. ¹H NMR (600 MHz, DMSO-*d*₆): δ 0.83 (s, 9H, (CH₃)₃), 1.25 (tt, *J*=11.1, 3.1 Hz, 1H, >CH-), 1.38 (qd, *J*=13.3, 4.0 Hz, 2H) and 1.74 (dm, 2H) (2× -CH₂-), (2.75 td, *J*=13.3, 2.8 Hz, 2H) and 3.26 (dm, 2H) (2× N-CH₂-), 8.72 (b, 2H, >NH₂). ¹³C NMR (150.9 MHz, DMSO-*d*₆): δ 23.56 (2× -CH₂-), 27.05 ((CH₃)₃), 32.16 (>C<), 43.61 (>CH-), 43.94 (2× N-CH₂). HRMS (ESI): [M+H]⁺, found 142.15892. C₉H₂₀N requires 142.15903.

4.5.2. N-Methyl-4-tert-butylpiperidine (4). 4-tert-Butylpiperidine hydrochloride (**2**) (11.5 g 64.7 mmol) was partitioned between Et₂O (2×200 mL) and 5 M aq NaOH (200 mL), the organic layer was dried

Table 4
Overview of the MAE_{oxid} values of oxidation induced NMR shifts for different calculation methods. The lowest MAE values are highlighted by yellow or green color

$$MAE_{oxid} = \frac{1}{n} \sum_{i=1}^n |\Delta\delta_{calc} - \Delta\delta_{exp}|$$

OPT	NMR	¹³ C [ppm]					¹ H [ppm]				
		N NO	P PO	S SO SO ₂	Se SeO SeO ₂	Average a	N NO	P PO	S SO SO ₂	Se SeO SeO ₂	Average a
B3LYP/6-31G*	B3LYP/6-31G*	1.19	0.38	0.50	1.78	0.96	0.19	0.29	0.16	0.19	0.21
B3LYP/6-31G* ^b	B3LYP/6-31G*	1.00	0.42	0.78	1.87	1.02	0.18	0.28	0.17	0.20	0.21
B3LYP/6-31G*	B3LYP/6-31G* ^b	1.19	1.03	0.44	1.67	1.08	0.14	0.27	0.12	0.15	0.17
B3LYP/6-31G* ^b	B3LYP/6-31G* ^b	1.00	0.42	0.57	1.75	0.94	0.14	0.27	0.11	0.14	0.16
B3LYP/6-31G*	OPBE/6-31G*	1.52	0.45	1.21	2.28	1.36	0.16	0.27	0.16	0.17	0.19
HF/6-31G*	HF/6-31G*	0.56	0.73	1.52	3.31	1.53	0.22	0.27	0.24	0.18	0.23
B3LYP/6-31G*	HF/6-31G*	0.59	0.70	0.91	4.10	1.58	0.21	0.26	0.12	0.14	0.18
B3LYP/6-31G*	OPBE/6-311G*	0.94	0.37	0.93	2.90	1.28	0.17	0.28	0.16	0.25	0.21
B3LYP/6-31G*	OPBE/6-31G**	1.19	0.45	1.20	2.63	1.37	0.17	0.25	0.16	0.22	0.20
B3LYP/6-31G**	B3LYP/6-31G**	1.26	1.17	0.52	2.42	1.34	0.18	0.28	0.19	0.21	0.22
B3LYP/6-311G**	B3LYP/6-311G**	1.15	0.27	0.44	1.13	0.75	0.18	0.29	0.18	0.23	0.22
B3LYP/6-311G** ^b	B3LYP/6-311G**	0.94	0.27	0.38	1.19	0.70	0.17	0.27	0.18	0.22	0.21
B3LYP/6-311G**	B3LYP/6-311G** ^b	1.31	0.18	0.52	0.93	0.74	0.14	0.26	0.13	0.17	0.17
B3LYP/6-311G** ^b	B3LYP/6-311G** ^b	0.95	0.19	0.34	0.99	0.62	0.13	0.27	0.12	0.16	0.17
B3LYP/6-31G**	B3LYP/6-31++G**	0.78	0.57	1.34	1.79	1.12	0.23	0.18	0.22	0.26	0.22
HF/6-311++G**	HF/6-311++G**	0.55	1.00	1.22	3.78	1.64	0.23	0.23	0.16	0.25	0.22
MP2/6-311++G**	HF/6-311++G**	1.67	0.54	0.17	3.96	1.51	0.83	0.22	0.15	0.24	0.36
MP2/6-311++G**	MP2/6-311++G**	1.24	1.01	0.59	3.04	1.47	0.76	0.49	0.22	0.29	0.44

^a MAE_{oxid} for all studied heterocycles; ^b PCM model, solvent = chloroform.

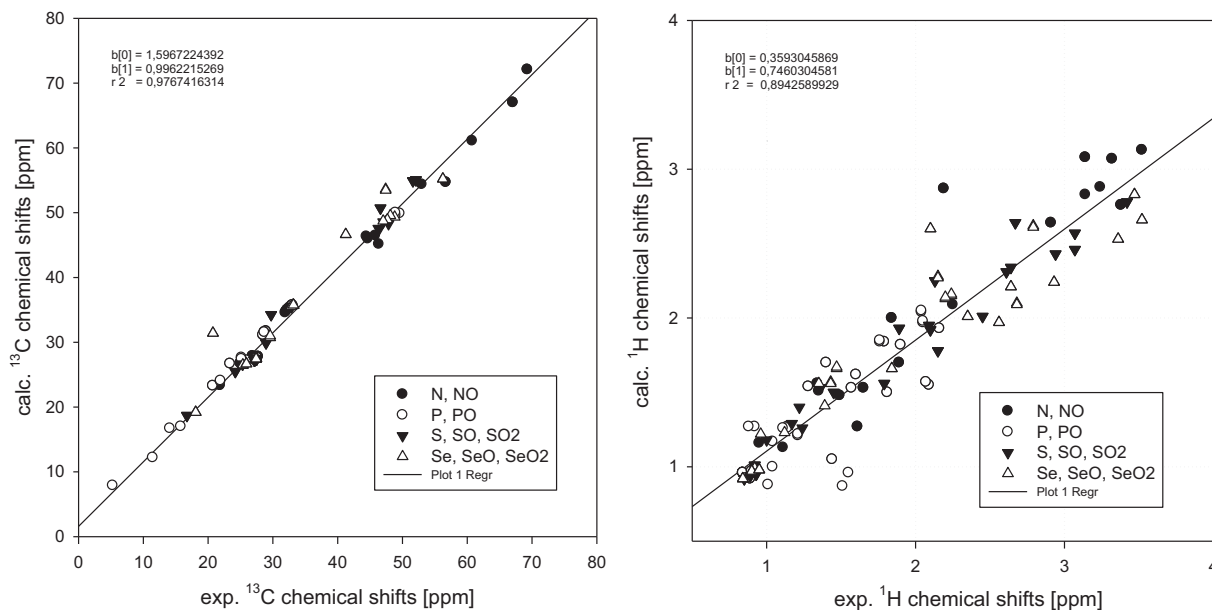


Fig. 9. The correlation of the experimental and calculated ¹³C (left) and ¹H (right) chemical shifts (OPT and NMR using DFT B3LYP 6-31G*) in all studied heterocycles.

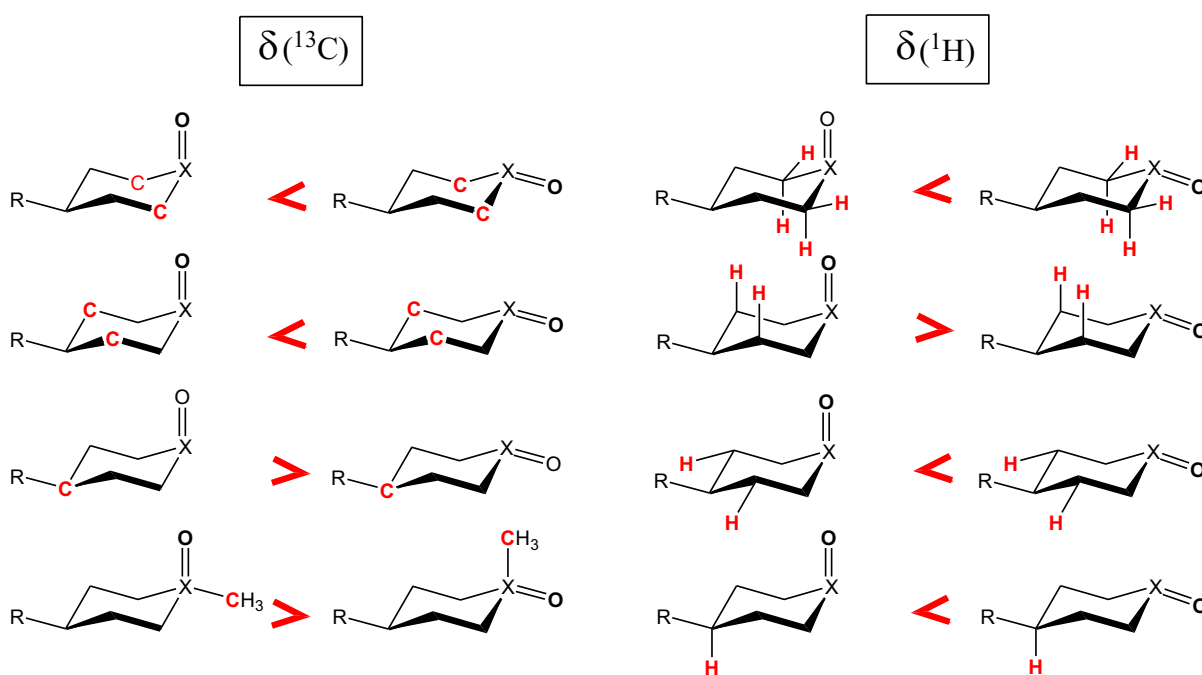
over Na₂SO₄, and the solvent evaporated in vacuo to give amine **3** as a slightly yellow liquid with a faint amine odor (8.89 g, 62.94 mmol, 97%). ¹H NMR (600 MHz, CDCl₃): δ 0.85 (s, 9H, (CH₃)₃), 1.08 (tt, J=11.9, 3.0 Hz, 1H, >CH-), 1.17 (qd, J=12.0, 4.0 Hz, 2H) and 1.66 (dm, 2H) (2 × -CH₂-), 2.05 (b, 1H, >NH), 2.55 (td, J=12.0, 2.6 Hz, 2H) and

3.12 (dm, 2H) (2 × N-CH₂-). ¹³C NMR (150.9 MHz, CDCl₃): δ 27.17 ((CH₃)₃), 27.92 (2 × -CH₂-), 32.28 (>C<), 46.88 (>CH-), 47.45 (2 × N-CH₂).

To a solution of **3** (8.89 g, 62.94 mmol) in water (38.0 mL) in a flask equipped with magnetic stirrer and a reflux condenser 98%

Table 5Comparison of the experimental and calculated (GIAO, B3LYP-6-31G*) ^1H and ^{13}C chemical shifts and oxidation induced shifts. The calculated values are given in brackets

Atom		NO (ax)	NO (eq)	PO (ax)	PO (eq)	SO (ax)	SO (eq)	SeO (ax)	SeO (eq)
<i>Chemical shifts [ppm]</i>									
C-2,6	Exp. calcd	67.05 (67.02)	69.28 (72.10)	28.46 (31.10)	28.68 (31.59)	46.61 (50.71)	52.08 (55.07)	41.24 (46.62)	47.40 (53.62)
C-3,5	Exp. calcd	21.84 (23.36)	24.97 (26.77)	21.93 (23.94)	25.16 (27.66)	16.74 (18.70)	24.20 (25.49)	18.07 (19.20)	25.36 (26.44)
C-4	Exp. calcd	44.65 (45.98)	44.43 (46.35)	48.92 (50.02)	47.86 (48.78)	47.03 (48.57)	46.41 (47.50)	48.12 (49.56)	47.66 (48.91)
X-CH ₃	Exp. calcd	60.76 (61.11)	52.99 (54.38)	15.79 (17.02)	11.45 (12.71)	—	—	—	—
H-2ax	Exp. calcd	3.14 (3.08)	3.32 (3.07)	1.44 (1.05)	1.81 (1.50)	2.45 (2.01)	2.61 (2.31)	2.56 (1.97)	2.68 (2.10)
H-2eq	Exp. calcd	3.38 (2.76)	3.52 (3.13)	2.09 (1.55)	2.07 (1.57)	3.07 (2.46)	3.42 (2.78)	2.93 (2.24)	3.47 (2.83)
H-3ax	Exp. calcd	2.19 (2.87)	1.49 (1.48)	2.06 (1.97)	1.21 (1.21)	2.13 (2.25)	1.45 (1.50)	2.10 (2.60)	1.43 (1.57)
H-3eq	Exp. calcd	1.61 (1.37)	1.89 (1.70)	1.76 (1.84)	2.16 (1.93)	1.79 (1.56)	2.10 (1.92)	1.84 (1.66)	2.20 (2.13)
H-4	Exp. calcd	1.11 (1.13)	1.35 (1.51)	1.04 (1.17)	1.11 (1.26)	1.17 (1.29)	1.22 (1.40)	1.12 (1.23)	1.35 (1.56)
X-CH ₃	Exp. calcd	3.24 (2.88)	3.14 (2.83)	1.51 (0.87)	1.55 (0.96)	—	—	—	—
<i>Oxidation induced shifts [ppm]</i>									
C-2,6	Exp. calcd	10.36 (12.32)	12.59 (17.40)	-0.49 (-0.64)	5.29 (4.88)	16.89 (16.44)	22.36 (20.80)	20.50 (15.21)	26.66 (22.21)
C-3,5	Exp. calcd	-5.02 (-4.49)	-1.89 (-1.08)	-3.98 (-3.15)	4.43 (4.37)	-12.20 (-11.20)	-4.74 (-4.41)	-11.50 (-11.52)	-4.21 (-4.28)
C-4	Exp. calcd	-1.16 (-0.49)	-1.38 (-0.12)	-0.66 (0.12)	-1.09 (-0.85)	-0.82 (0.29)	-1.44 (-0.78)	-0.68 (0.23)	-1.14 (-0.42)
X-CH ₃	Exp. calcd	14.41 (15.95)	6.64 (9.22)	1.69 (0.30)	6.18 (4.30)	—	—	—	—
H-2ax	Exp. calcd	1.30 (1.08)	1.48 (1.07)	0.30 (-0.22)	0.21 (-0.12)	-0.22 (-0.63)	-0.06 (-0.33)	-0.23 (-0.65)	-0.11 (-0.52)
H-2eq	Exp. calcd	0.47 (0.12)	0.61 (0.49)	0.19 (-0.27)	0.50 (0.04)	0.43 (0.12)	0.78 (0.44)	0.29 (0.03)	0.83 (0.62)
H-3ax	Exp. calcd	0.85 (1.31)	0.15 (-0.08)	0.77 (0.43)	-0.19 (-0.49)	0.77 (0.72)	0.09 (-0.03)	0.63 (0.94)	-0.04 (-0.09)
H-3eq	Exp. calcd	-0.04 (-0.26)	0.24 (0.17)	-0.28 (-0.20)	0.37 (0.09)	-0.30 (-0.39)	0.01 (-0.03)	-0.40 (-0.49)	-0.04 (-0.02)
H-4	Exp. calcd	0.16 (-0.03)	0.40 (0.35)	0.12 (-0.10)	0.23 (-0.01)	0.17 (0.11)	0.22 (0.22)	0.16 (0.01)	0.39 (0.34)
X-CH ₃	Exp. calcd	0.99 (0.79)	0.89 (0.74)	0.50 (-0.01)	0.51 (-0.04)	—	—	—	—

**Fig. 10.** General rules for relations between ^{13}C and ^1H chemical shifts of carbon and hydrogen atoms in different positions of O(ax) and O(eq) stereoisomers.

formic acid (13.00 mL, 338 mmol, 5.4 equiv) and formaldehyde (37% aq solution, 8.80 mL, 118.2 mmol, 1.88 equiv) were added, and the reaction mixture was heated to reflux for 18 h. After cooling, the reaction mixture was made strongly alkaline with 50% aqueous NaOH and the crude product was extracted with diethyl ether (3×100 mL). The combined organic phase was dried over anhydrous sodium sulfate, and the solvent was removed in vacuo at 30 °C. The oily residue was dissolved in 9:1 (v/v) MeOH–water mixture and passed through a column of Dowex 50 (H⁺-cycle), the column was washed successively with water, methanol and again water. The crude product was eluted with 10% aq NH₃ and the aqueous solution was distilled in vacuo at 55 °C. The distillate was acidified by hydrochloric acid to pH 4, evaporated to dryness, the free amine was released by adding 10 M aq NaOH (50 mL),

extracted to diethyl ether (3×50 mL) and dried over anhydrous sodium sulfate. Removing the solvent in vacuo at 25 °C afforded the target amine **4** as pale yellow oil with a faint odor (6.185 g, 39.8 mmol, 63%; density 0.83 g/mL, *R_f* 0.5 in H1).

^1H and ^{13}C NMR data—see Fig. 2, ^{15}N NMR data in Fig. 3. HRMS (ESI): [M+H]⁺, found 156.17466. C₁₀H₂₂N requires 156.17468.

4.5.3. N-Methyl-4-tert-butylpiperidine N-oxide (5). To a solution of **4** (0.124 g, 0.798 mmol) in methanol (5 mL) hydrogen peroxide (30% aq solution, 5 mL) was added and the stirred reaction mixture was heated to 45 °C for 24 h. After the reaction was complete, the excess H₂O₂ was decomposed by adding 10% palladium on charcoal (10 mg) and stirring the suspension for 1 h. The reaction mixture was filtered through Celite and evaporated in vacuo at 50 °C to

afford the target *N*-oxide **5** as a white solid (0.134 g, 0.78 mmol, 98%; R_f 0.15 in H1). ^1H and ^{13}C NMR data—see Fig. 2, ^{15}N NMR data in Fig. 3. HRMS (ESI): $[\text{M}+\text{H}]^+$, found 172.16960. $\text{C}_{10}\text{H}_{22}\text{ON}$ requires 172.16959.

4.5.4. *N*-Benzoyl-4-*tert*-butylpiperidine (6**).** To a solution of hydrochloride **2** (95.57 g, 0.537 mol) in water (500 mL) in a 2 L round-bottomed flask equipped with a magnetic stirrer and dropping funnel and cooled in an ice bath a solution of NaOH (49.49 g, 1.23 mol, 2.3 equiv) in water (100 mL) was added. Then, benzoyl chloride (62.47 mL, 0.537 mol, 1 equiv) diluted with diethyl ether (100 mL to prevent lumping of crude product) was slowly added from the dropping funnel to an intensively stirred reaction mixture. After 12 h at room temperature, the mixture was partitioned between water and Et₂O (500 mL, then 2 × 150 mL), and the organic layer was dried over Na₂SO₄ and evaporated in vacuo. The crude product was purified by flash chromatography on silica (elution with a linear gradient of EtOAc in toluene) to give compound **6** as white glistening crystals (129.5 g, 528 mmol, 98%; R_f 0.75 in T1). ^1H NMR (600 MHz, CDCl₃): δ 0.87 (s, 9H, (CH₃)₃), 1.26 (tt, $J=11.8$, 2.9 Hz, 1H, >CH–), 1.17 (bt, $J\sim 11$ Hz, 1H) and 1.63 (bd, $J\sim 11$ Hz, 1H) (–CH₂–), 1.30 (bt, $J\sim 11$ Hz, 1H) and 1.82 (bd, $J\sim 11$ Hz, 1H) (–CH₂–), 2.66 (bt, $J\sim 11$ Hz, 1H) and 4.81 (bd, $J\sim 11$ Hz, 1H) (N–CH₂–), 2.93 (bt, $J\sim 11$ Hz, 1H) and 3.80 (bd, $J\sim 11$ Hz, 1H) (N–CH₂–), 7.40 (m, 5H, C₆H₅). ^{13}C NMR (150.9 MHz, CDCl₃): δ 27.23 ((CH₃)₃), 26.64 (–CH₂–), 27.59 (–CH₂–), 32.24 (>C<), 42.99 (N–CH₂–), 46.81 (>CH–), 48.59 (N–CH₂–), 126.84 (2 × *o*-ArC), 128.35 (2 × *m*-ArC), 129.36 (*p*-ArC), 136.38 (*i*-ArC), 170.10 (>C=O). HRMS (ESI): $[\text{M}+\text{H}]^+$, found 246.18515. $\text{C}_{16}\text{H}_{24}\text{ON}$ requires 246.18524.

4.5.5. 4-*tert*-Butyl-1,5-dibromopentane (7**).** *N*-Benzoyl-4-*tert*-butylpiperidine (**6**) (129.5 g, 528 mmol) was placed in a three-necked round-bottomed flask equipped with mechanical stirrer and addition funnel. Phosphorus tribromide (49.9 mL, 531 mmol, 1 equiv) was added dropwise over a 30-min period at room temperature. After stirring at rt for 2 h, the light yellow liquid was cooled with an ice bath, followed by dropwise addition of bromine (27.2 mL, 531 mmol, 1 equiv) over the course of 30 min. After 1 h, the resulting black viscous oil was heated to 150 °C for 12 h. Upon cooling to room temperature, a mass of crystalline POBr₃ precipitated; the mixture was diluted with 500 mL of acetonitrile, and the crystals were quickly filtered off through a fritted filtration funnel. The black filtrate was extracted with hexane (2 × 300 mL, then 10 × 100 mL), the combined organic layers were washed successively with water (300 mL) and saturated aq NaHCO₃ (300 mL), and the total volume was reduced to 0.5 L in vacuo. Then, benzonitrile was removed by extracting with conc. H₂SO₄ (10 × 50 mL), the pale yellow hexane layer was washed with water (200 mL) and saturated aq NaHCO₃ (200 mL), dried over Na₂SO₄, and evaporated in vacuo to give 51.85 g of crude product. Distillation under reduced pressure afforded 41.1 g (144 mmol, 27.2%) of dibromide **7** as a colorless liquid (bp 85–90 °C/2 Torr, density 1.41 g/mL, R_f 0.8 in HT). ^1H NMR (600 MHz, CDCl₃): δ 0.90 (s, 9H, (CH₃)₃), 1.24 (tt, $J=7.3$, 3.7 Hz, 1H, >CH–), 1.62 (dddd, $J=14.5$, 8.4, 7.3, 5.6 Hz, 2H) and 2.09 (dddd, $J=14.5$, 8.8, 7.3, 3.7 Hz, 2H) (2 × –CH₂–), 3.40 (ddd, $J=9.9$, 8.4, 5.6 Hz, 2H) and 3.49 (ddd, $J=9.9$, 8.8, 5.6 Hz, 2H) (2 × –CH₂–Br). ^{13}C NMR (150.9 MHz, CDCl₃): δ 27.49 ((CH₃)₃), 33.15 (2 × –CH₂–Br), 33.72 (>C<), 34.95 (2 × –CH₂–), 46.52 (>CH–). HRMS (ESI): $[\text{M}+\text{H}]^+$, found 286.98339. $\text{C}_9\text{H}_{19}\text{Br}_2$ requires 286.98330.

4.5.6. 4-*tert*-Butyl-1-hydroxyphosphorinane 1-oxide (8**).** To a three-necked round-bottomed flask equipped with magnetic stirrer, argon inlet and a reflux condenser dibromide **7** (10.0 g, 35 mmol) was placed, dry ammonium hypophosphite (11.6 g, 140 mmol, 4 equiv), hexamethyldisilazane (58.4 mL, 280 mmol, 8 equiv) and mesitylene (120 mL) were added, and the reaction mixture was heated to

160 °C for 12 h under a steady flow of argon to dilute the emerging highly pyrophoric bistrimethylsilyl phosphonite (BTSP). The dark-brown mixture was then cooled to room temperature, the reaction was quenched by adding 2 M aqueous HCl (50 mL), filtered through Celite, and the filtration cake was washed with EtOAc (200 mL). The filtrate was diluted with water (500 mL), and the product was extracted with EtOAc (4 × 200 mL). The combined organic phase was dried over anhydrous sodium sulfate, filtered again, and the solvents were removed in vacuo at 80 °C to give the desired phosphinic acid **8** as a pale yellow semisolid (3.65 g, 19.19 mmol, 54%; 42–55 % in repeated runs, R_f 0.15 in H1). ^1H NMR (600 MHz, CDCl₃): δ 0.88 (s, 9H, (CH₃)₃), 1.03 (tm, 1H, >CH–), 1.54 (m, 2H) and 2.07 (m, 2H) (2 × –CH₂–), 1.61 (m, 2H) and 1.98 (m, 2H) (2 × P–CH₂–), 10.15 (br s, 1H, P–OH). ^{13}C NMR (150.9 MHz, CDCl₃): δ 24.54 (d, $^2J(\text{P,C})=5.2$ Hz, 2 × –CH₂–), 27.70 (d, $^1J(\text{P,C})=87.6$ Hz, 2 × P–CH₂–), 27.72 ((CH₃)₃), 32.82 (d, $^4J(\text{P,C})=0.9$ Hz, >C<), 48.26 (d, $^3J(\text{P,C})=5.0$ Hz, >CH–). HRMS (ESI): $[\text{M}+\text{H}]^+$, found 191.11970. $\text{C}_9\text{H}_{20}\text{O}_2\text{P}$ requires 191.11954.

4.5.7. 4-*tert*-Butyl-1-chlorophosphorinane 1-oxide (9**).** To a solution of phosphinic acid **8** (4.0 g, 21.0 mmol) and a catalytic amount of DMF (200 μL) in dichloromethane (60 mL) in a flask equipped with magnetic stirrer and cooled in an ice bath, oxalyl chloride (3.61 mL, 42.1 mmol, 2 equiv) in CH₂Cl₂ (20 mL) was slowly added from the dropping funnel with constant stirring. After the addition was complete, the mixture was allowed to warm to room temperature and stir for an additional 2 h. The solution was then evaporated in vacuo to give brown crystalline mass of crude **9** (epimeric mixture, **9a**:**9b** = 80:20 by NMR), which was used in the next step without further purification. Major epimer **9a**: ^1H NMR (600 MHz, CDCl₃): δ 0.91 (s, 9H, (CH₃)₃), 1.11 (m, 1H, >CH–), 1.59 (m, 2H) and 2.16 (m, 2H) (2 × –CH₂–), 2.12 (m, 2H) and 2.38 (m, 2H) (2 × P–CH₂–). ^{13}C NMR (150.9 MHz, CDCl₃): δ 25.04 (d, $^2J(\text{P,C})=5.7$ Hz, 2 × –CH₂–), 27.59 ((CH₃)₃), 32.74 (d, $^4J(\text{P,C})=1.2$ Hz, >C<), 33.56 (d, $^1J(\text{P,C})=69.2$ Hz, 2 × P–CH₂–), 47.80 (d, $^3J(\text{P,C})=5.2$ Hz, >CH–). Minor epimer **9b**: ^1H NMR (600 MHz, CDCl₃): δ 0.91 (s, 9H, (CH₃)₃), 1.20 (m, 1H, >CH–), 1.82 (m, 2H) and 2.13 (m, 2H) (2 × –CH₂–), 1.99 (m, 2H) and 2.50 (m, 2H) (2 × P–CH₂–). ^{13}C NMR (150.9 MHz, CDCl₃): δ 24.51 (d, $^2J(\text{P,C})=5.8$ Hz, 2 × –CH₂–), 26.56 ((CH₃)₃), 32.95 (d, $^4J(\text{P,C})=1.0$ Hz, >C<), 34.80 (d, $^1J(\text{P,C})=70.3$ Hz, 2 × P–CH₂–), 48.22 (d, $^3J(\text{P,C})=4.6$ Hz, >CH–).

4.5.8. 4-*tert*-Butyl-1-methylphosphorinane 1-oxide (10**).** To a solution of crude chloride **9** (assumed 21 mmol) in diethyl ether (40 mL) in a flask equipped with a magnetic stirrer, reflux condenser and argon inlet, CH₃MgBr (3 M solution in Et₂O; 21.02 mL, 63 mmol, 3 equiv) was added via syringe through a rubber septum with spontaneous reflux. After the addition was complete, the solution was heated to reflux for 2 h. The reaction mixture was then diluted with CH₂Cl₂ (200 mL) and poured slowly into a vigorously stirred 0.5 M aqueous HCl (200 mL). The dichloromethane layer was separated, the aqueous layer was extracted with additional dichloromethane (2 × 100 mL), the combined organic phase was washed with saturated aq NaHCO₃ (100 mL), dried over Na₂SO₄ and evaporated in vacuo. The crude product was recrystallized from hexane-EtOAc mixture to give phosphin oxide **10** as pale brown needles (2.02 g, 10.74 mmol, 51% over two steps; R_f 0.5 in H3. Colorless needles when obtained by oxidation of phosphine **11**). ^1H and ^{13}C NMR data—see Fig. 4; ^{31}P NMR data—see Fig. 5. HRMS (ESI): $[\text{M}+\text{H}]^+$, found 189.14080. $\text{C}_{10}\text{H}_{22}\text{OP}$ requires 189.14083.

4.5.9. 4-*tert*-Butyl-1-methylphosphorinane (11**).** To the phosphin oxide **10** (1.0 g, 5.31 mmol) in a flask equipped with reflux condenser and argon inlet, phenyl silane (0.44 mL, 3.56 mmol, 0.67 equiv) was added via syringe through a rubber septum. The mixture became homogenous in 5 min, and an exothermic reaction

started, accompanied with evolution of hydrogen. The reaction mixture was heated to 80 °C under reflux for 5 h. The reflux was then stopped, and a stream of argon was blown through the reaction flask to a trap cooled to –78 °C, affording the target phosphine **11** as a colorless liquid (0.190 g, 1.1 mmol, 21%). ¹H and ¹³C NMR data—see Fig. 4; ³¹P NMR data—see Fig. 5. HRMS (ESI): [M+H]⁺, found 173.14534. C₁₀H₂₂P requires 173.14536.

4.5.10. 4-tert-Butylthiane (12) and 5-tert-butyl-1,2-dithiepane (13). To a three-necked round-bottomed flask equipped with mechanical stirrer, reflux condenser and two addition funnels DMF (120 mL) was placed and heated to 90 °C under argon atmosphere. A solution of dibromide **7** (10.0 g, 35.0 mmol, in 30 mL of DMF) and a solution of sodium sulfide nonahydrate (9.236 g, 38.5 mmol, 1.1 equiv in 30 mL of 1:1 (v/v) water-DMF mixture) were added simultaneously dropwise to an intensively stirred DMF over a period of 20 min. Stirring and heating was continued under argon atmosphere for 12 h, the dark-brown reaction mixture was then cooled to room temperature, and the crude product was extracted with hexane (3×100 mL). The combined hexane phase was dried over anhydrous sodium sulfate, and the hexane was removed in vacuo at 30 °C. The dark red-brown oil residue was purified by flash chromatography on silica (elution with hexane, isocratic) to give 4-tert-butylthiane **12** as a pale yellow liquid with a distinctive pungent odor (3.105 g, 19.6 mmol, 56%; R_f 0.7 in HT, density 0.92 g/mL) and 5-tert-butyl-1,2-dithiepane **13** as a colorless liquid with camphorous odor (0.321 g, 1.69 mmol, 4.8%; R_f 0.8 in HT, density 1.03 g/mL).

4.5.10.1. 4-tert-Butylthiane 12. ¹H and ¹³C NMR data—see Fig. 6. HRMS (EI): found 190.0851. C₉H₁₈S requires 190.0850.

4.5.10.2. 5-tert-Butyl-1,2-dithiepane 13. ¹H NMR (150.9 MHz, CDCl₃): δ 0.90 (s, 9H, (CH₃)₃), 1.46 (tt, J=8.2, 1.8 Hz, 1H, >CH–), 1.69 (dddd, J=14.6, 12.6, 8.2, 4.4 Hz, 2H) and 2.18 (dddd, J=14.6, 4.0, 3.1, 1.8 Hz, 2H) (2× –CH₂–), 2.51 (ddd, J=13.0, 12.6, 4.0 Hz, 2H) and 3.04 (ddd, J=13.0, 4.4, 3.1 Hz, 2H) (2× S–CH₂–). ¹³C NMR (150.9 MHz, CDCl₃): 27.09 ((CH₃)₃), 31.81 (2× –CH₂–), 34.03 (>C<), 38.28 (2× S–CH₂–), 47.35 (>CH–). HRMS (EI): found 158.1126. C₉H₁₈S₂ requires 158.1129.

4.5.11. 4-tert-Butylthiane 1-oxide (14) and 4-tert-butylthiane 1-dioxide (15). To a solution of sulfide **12** (0.184 g, 1.16 mmol) in dioxane (1 mL) 30% aqueous hydrogen peroxide (0.142 mL, 1.39 mmol, 1.2 equiv) was added, and the solution was stirred at room temperature for 2 d. The reaction mixture was then evaporated in vacuo, co-distilled with EtOH (2 mL), and the residue was purified by flash chromatography on silica (elution with a linear gradient of EtOH in CHCl₃) to give 4-tert-butylthiane-1-oxide (**14**) as colorless hygroscopic crystals (0.187 g, 1.1 mmol, 92%; R_f 0.6 in C1). Small amount (~5%) of 4-tert-butylthiane-1-dioxide (**15**) was detected as the admixture in NMR spectra. ¹H and ¹³C NMR data—see Fig. 6. HRMS (ESI): [M+H]⁺, found 175.11505. C₉H₁₉OS requires 175.11511.

4.5.12. 4-tert-Butylselenane (16). To a suspension of selenium (2.015 g, 25.5 mmol, 1.46 equiv) in H₂O (300 mL), containing a small amount of EtOH (10 mL) to facilitate wetting, sodium borohydride (2.095 g, 55.4 mmol, 3.17 equiv) was added and the mixture was stirred at room temperature until the solution became clear (ca. 10 min). A solution of dibromide **7** (5.0 g, 17.5 mmol, in 100 mL of dioxane) was added and the reaction mixture was heated to 100 °C under argon atmosphere for 3 days. The reaction was then cooled to room temperature, diluted with water (500 mL) and the crude product was extracted with hexane (3×100 mL). The combined hexane phase was dried over anhydrous sodium sulfate, and the

hexane was removed in vacuo at 30 °C. The pale yellow oil residue was purified by flash chromatography on silica (elution with a linear gradient of toluene in hexane) to give 4-tert-butylselenane **16** as a pale yellow liquid (density 1.18 g/mL) with a distinctive odor (3.34 g, 16.3 mmol, 93%; R_f 0.7 in HT). ¹H and ¹³C NMR data—see Fig. 7; ⁷⁷Se NMR data—see Fig. 8. HRMS (EI): found 206.0574. C₉H₁₈Se requires 206.0577.

4.5.13. 4-tert-Butylselenane 1-oxide trifluoroacetate (17). To a solution of selenide **16** (0.359 g, 1.75 mmol) in 3:1:0.2 (v/v) MeOH-dioxane-water mixture (4.2 mL) sodium periodate (0.561 g, 2.62 mmol, 1.5 equiv) was added and the solution was stirred at room temperature for 1 h. The precipitated salts were then filtered off, the filtrate was evaporated in vacuo, dissolved in CHCl₃ (10 mL) and filtered again to remove remaining inorganic salts. The filtrate was evaporated, and the residue was purified by HPLC (see Section 4.1.) to afford, after recrystallization from THF-hexane, the title compound **17** as colorless needles (0.175 g, 0.52 mmol, 30%; mp 106–107 °C, R_f 0.2 in H1). ¹H NMR (600 MHz, CDCl₃): δ 0.92 (s, 9H, (CH₃)₃), 1.23 (tt, J=11.2, 3.3 Hz, 1H, >CH–), 1.98 (m, 2H) and 2.02 (m, 2H) (2× –CH₂–), 3.05 (td, J=13.1, 4.4 Hz, 2H) and 3.46 (dm, 2H) (2× Se–CH₂–). ¹³C NMR (150.9 MHz, CDCl₃): δ 18.95 (2× –CH₂–), 27.14 ((CH₃)₃), 33.18 (>C<), 40.64 (2× Se–CH₂–), 46.59 (>CH–). HRMS (ESI): [M+H]⁺, found 223.05959. C₉H₁₉OSe requires 223.05956.

4.5.14. 4-tert-Butylselenane 1-oxide periodate (18). To a solution of selenide **16** (0.236 g, 1.15 mmol) in 3:1:0.2 (v/v) MeOH-dioxane-water mixture (4.2 mL) sodium periodate (0.369 g, 1.72 mmol, 1.5 equiv) was added, and the solution was stirred at room temperature for 1 h. Anhydrous Na₂SO₄ (2 g) was then added, the reaction mixture was diluted with CHCl₃ (50 mL) and stirred for 0.5 h. The precipitated salts were filtered off, the filtrate was evaporated in vacuo, dissolved in benzene (10 mL) and filtered again to remove remaining inorganic salts. The filtrate was evaporated, and the residue was recrystallized from benzene-hexane system at –20 °C to furnish the title compound as white solid (0.195 g, 0.47 mmol, 41%; R_f 0.2 in H1). A small portion of the product was recrystallized from THF-hexane to give colorless needles of **18** (mp 127–128 °C). ¹H NMR (600 MHz, D₂O): δ 0.88 (s, 9H, (CH₃)₃), 1.28 (tt, J=11.8, 2.4 Hz, 1H, >CH–), 1.78 (dddd, J=15.1, 13.6, 11.8, 3.0 Hz, 2H) and 1.97 (dm, 2H) (2× –CH₂–), 2.96 (td, J=13.6, 3.5 Hz, 2H) and 3.14 (dm, 2H) (2× Se–CH₂–). ¹³C NMR (150.9 MHz, D₂O): δ 21.43 (2× –CH₂–), 29.35 ((CH₃)₃), 35.27 (>C<), 43.52 (2× Se–CH₂–), 49.00 (>CH–). HRMS (ESI): [M+H]⁺, found 223.05945. C₉H₁₉OSe requires 223.05956.

4.5.15. 4-tert-Butylselenane 1-oxide (19). To a solution of selenide **16** (0.236 g, 1.15 mmol) in dioxane (1.0 mL) 30% H₂O₂ (0.117 mL, 1.15 mmol, 1 equiv) was added and the solution was stirred at room temperature for 12 h. The reaction mixture was then evaporated in vacuo at 25 °C affording white solid, which was recrystallized from THF-hexane to give selenoxide **19** (as epimeric mixture, **19a:19b**=82:18 by NMR) as colorless glistening platelets (0.214 g, 0.97 mmol, 84%; mp 126–127 °C, R_f 0.3 in H1). ¹H and ¹³C NMR data—see Fig. 7; ⁷⁷Se NMR data—see Fig. 8. HRMS (ESI): [M+H]⁺, found 223.05952. C₉H₁₉OSe requires 223.05956.

4.5.16. 4-tert-Butylselenane 1,1-dioxide (20)

4.5.16.1. Method A. To a solution of selenide **16** (0.175 g, 0.85 mmol) in 1:1 (v/v) H₂O–CH₂Cl₂ mixture (5.0 mL) finely crushed KMnO₄ (0.202 g, 1.28 mmol, 1.5 equiv) was added and the reaction mixture was stirred at room temperature for 12 h. The solution was diluted with isopropanol (50 mL) and stirring was continued for another 2 h at room temperature; the solid precipitate was then filtered off, and the filtrate was evaporated in vacuo. The solid residue was dissolved in CHCl₃ (10 mL), the

solution was filtered and evaporated to give selenone **20** as a white solid (0.185 g, 0.78 mmol, 91%; R_f 0.7 in H₃).

4.5.16.2. Method B. Selenide **16** (0.236 g, 1.15 mmol) was added to excess 30% aq H₂O₂ (2 mL) and the reaction mixture was vigorously stirred at room temperature for 12 h. The product was extracted with CH₂Cl₂ (3 × 2 mL), the combined organic phase was dried over anhydrous sodium sulfate, and the solvent was removed in vacuo at 30 °C. The solid residue was recrystallized from THF to give selenone **20** as colorless glistening crystals (0.232 g, 0.98 mmol, 85%; mp 225 °C). ¹H and ¹³C NMR data—see Fig. 7; ⁷⁷Se NMR data—see Fig. 8. HRMS (ESI): [M+Na]⁺, found 261.03645. C₉H₁₈O₂NaSe requires 261.03642.

Acknowledgements

This work was supported by the Czech Science Foundation (Grant No. 203-09-1919 and 13-24880S).

Supplementary data

X-ray crystallographic data showing hydrogen-bonding network in crystals of compounds **19a** and **20** are available. Supplementary data related to this article can be found at <http://dx.doi.org/10.1016/j.tet.2014.04.047>.

References and notes

- Neuhaus, D.; Williamson, M. P. *The Nuclear Overhauser Effect in Structural and Conformational Analysis*; Wiley-VCH, 2000.
- Karplus, M. *J. Am. Chem. Soc.* **1963**, *85*, 2870–2871.
- Bifulco, G.; Dambruoso, P.; Gomez-Paloma, L.; Riccio, R. *Chem. Rev.* **2007**, *107*, 3744–3779.
- Smith, S. G.; Goodman, J. M. *J. Am. Chem. Soc.* **2010**, *132*, 12946–12959.
- Dracinsky, M.; Pohl, R.; Slavetinska, L.; Budesinsky, M. *Magn. Reson. Chem.* **2010**, *48*, 718–726; Dracinsky, M.; Pohl, R.; Slavetinska, L.; Hrebabecky, H.; Budesinsky, M. *Tetrahedron: Asymmetry* **2011**, *22*, 1797–1808; Dracinsky, M.; Pohl, R.; Slavetinska, L.; Janku, J.; Budesinsky, M. *Tetrahedron: Asymmetry* **2011**, *22*, 356–366.
- Pohl, R.; Dracinsky, M.; Slavetinska, L.; Budesinsky, M. *Magn. Reson. Chem.* **2011**, *49*, 320–327.
- Pohl, R.; Potmischil, F.; Dracinsky, M.; Vanek, V.; Slavetinska, L.; Budesinsky, M. *Magn. Reson. Chem.* **2012**, *50*, 415–423.
- Eliel, E. L.; Wilen, S. H.; Mander, L. N. *Stereochemistry of Organic Compounds*; John Wiley & Sons: New York, NY, 1994.
- Chambournier, G.; Gawley, R. E. *Org. Lett.* **2000**, *2*, 1561–1564 Gössinger, E. Beiträge zur Stereochemie der Additionsreaktionen an 3,4,5,6-Tetrahydropyridin-1-oxide. 2. Mitt., 1982; Vol. 113, pp 339–354.
- Wawzonek, S.; Nelson, M. F.; Thelen, P. *J. Am. Chem. Soc.* **1952**, *74*, 2894–2896; Bellamy, F. D.; Chazan, J. B.; Dodey, P.; Dutartre, P.; Ou, K.; Pascal, M.; Robin, J. J. *Med. Chem.* **1991**, *34*, 1545–1552.
- Harris, G. H.; Shelton, R. S.; Vancampen, M. G.; Andrews, E. R.; Schumann, E. L. *J. Am. Chem. Soc.* **1951**, *73*, 3959–3963; Crowley, P. J.; Robinson, M. J. T.; Ward, M. G. *Tetrahedron* **1977**, *33*, 915–925.
- Shvo, Y.; Kaufman, E. D. *J. Org. Chem.* **1981**, *46*, 2148–2152; Potmischil, F.; Duddeck, H.; Nicolescu, A.; Deleanu, C. *Magn. Reson. Chem.* **2007**, *45*, 231–235.
- Johnson, C. R.; McCants, D. *J. Am. Chem. Soc.* **1965**, *87*, 1109–1114.
- House, H. O.; Tefertiller, B. A.; Pitt, C. G. *J. Org. Chem.* **1966**, *31*, 1073–1079.
- Montchamp, J. L.; Tian, F.; Frost, J. W. *J. Org. Chem.* **1995**, *60*, 6076–6081.
- Tasz, M. K.; Gamliel, A.; Rodriguez, O. P.; Lane, T. M.; Cremer, S. E.; Bennett, D. W. *J. Org. Chem.* **1995**, *60*, 6281–6288.
- Marsi, K. L.; Jasperse, J. L.; Llort, F. M.; Kanne, D. B. *J. Org. Chem.* **1977**, *42*, 1306–1311.
- Szczepina, M. G.; Johnston, B. D.; Yuan, Y.; Svensson, B.; Pinto, B. M. *J. Am. Chem. Soc.* **2004**, *126*, 12458–12469.
- Braverman, S.; Cherkinsky, M.; Birska, M. L.; Zafrani, Y. *Eur. J. Org. Chem.* **2002**, 3198–3207.
- Procter, D. J.; Rayner, C. M. *Tetrahedron Lett.* **1994**, *35*, 1449–1452; Procter, D. J.; Thornton-Pett, M.; Rayner, C. M. *Tetrahedron* **1996**, *52*, 1841–1854.
- Paetzold, R.; Lindner, U.; Bochmann, G.; Reich, P. Z. *Anorg. Allg. Chem.* **1967**, *352*, 295–308.
- Krief, A.; Dumont, W.; Denis, J. N.; Evrard, G.; Norberg, B. *J. Chem. Soc., Chem. Commun.* **1985**, 569–570.
- Hommens, N.; Clark, T. *J. Mol. Model.* **2005**, *11*, 175–185.
- Frisch, M. J.; Trucks, G. W.; Schlegel, H. B.; Scuseria, G. E.; Robb, M. A.; Cheeseman, J. R.; Montgomery, J. A.; Vreven, T.; Kudin, K. N.; Burant, J. C.; Millam, J. M.; Iyengar, S. S.; Tomasi, J.; Barone, V.; Mennucci, B.; Cossi, M.; Scalmani, G.; Rega, N.; Petersson, G. A.; Nakatsuji, H.; Hada, M.; Ehara, M.; Toyota, K.; Fukuda, R.; Hasegawa, J.; Ishida, M.; Nakajima, T.; Honda, Y.; Kitao, O.; Nakai, H.; Klene, M.; Li, X.; Knox, J. E.; Hratchian, H. P.; Cross, J. B.; Bakken, V.; Adamo, C.; Jaramillo, J.; Gomperts, R.; Stratmann, R. E.; Yazyev, O.; Austin, A. J.; Cammi, R.; Pomelli, C.; Ochterski, J. W.; Ayala, P. Y.; Morokuma, K.; Voth, G. A.; Salvador, P.; Dannenberg, J. J.; Zakrzewski, V. G.; Dapprich, S.; Daniels, A. D.; Strain, M. C.; Farkas, O.; Malick, D. K.; Rabuck, A. D.; Raghavachari, K.; Foresman, J. B.; Ortiz, J. V.; Cui, Q.; Baboul, A. G.; Clifford, S.; Cioslowski, J.; Stefanov, B. B.; Liu, G.; Liashenko, A.; Piskorz, P.; Komaromi, I.; Martin, R. L.; Fox, D. J.; Keith, T.; Al-Laham, M. A.; Peng, C. Y.; Nanayakkara, A.; Challacombe, M.; Gill, P. M. W.; Johnson, B.; Chen, W.; Wong, M. W.; Gonzalez, C.; Pople, J. A. *Gaussian 03, Revision C.02*; Gaussian: Wallingford CT, 2004.